SEDIMENTOLOGY the journal of the International Association of Sedimentologists

Sedimentology (2015) doi: 10.1111/sed.12203

Back-flow ripples in troughs downstream of unit bars: Formation, preservation and value for interpreting flow conditions

CHRISTOPHER M. HERBERT, JAN ALEXANDER and MARÍA J. MARTÍNEZ DE ÁLVARO

School of Environmental Sciences, University of East Anglia, Norwich Research Park, Norwich, NR4 7TJ, UK (E-mail: christopher.herbert@uea.ac.uk)

ABSTRACT

Back-flow ripples are bedforms created within the lee-side eddy of a larger bedform with migration directions opposed or oblique to that of the host bedform. In the flume experiments described in this article, back-flow ripples formed in the trough downstream of a unit bar and changed with mean flow velocity; varying from small incipient back-flow ripples at low velocities, to well-formed back-flow ripples with greater velocity, to rapidly migrating transient back-flow ripples formed at the greatest velocities tested. In these experiments back-flow ripples formed at much lower mean back-flow velocities than predicted from previously published descriptions. This lower threshold mean back-flow velocity is attributed to the pattern of velocity variation within the lee-side eddy of the host bedform. The back-flow velocity variations are attributed to vortex shedding from the separation zone, wake flapping and increases in the size of, and turbulent intensity within, the flow separation eddy controlled by the passage of superimposed bedforms approaching the crest of the bar. Short duration high velocity packets, whatever their cause, may form back-flow ripples if they exceed the minimum bed shear stress for ripple generation for long enough or, if much faster, may wash them out. Variation in back-flow ripple cross-lamination has been observed in the rock record and, by comparison with flume observations, the preserved back-flow ripple morphology may be useful for interpreting formative flow and sediment transport dynamics.

Keywords Back-flow ripples, bedforms, bottomsets, counter-current ripples, ripples, ripple cross-lamination.

INTRODUCTION

Water flowing over non-cohesive sediments can form regular bed morphologies such as ripples, dunes and bars. Bedforms are controlled by parameters of the flow including velocity, shear stress and flow depth as well as the sediment characteristics. Bedforms modify the flow with flow separation generating lee-side eddies. Within lee-side eddies, the flow close to the bed travels in the opposite direction to the main flow (Fig. 1) or obliquely to it. In the lee of dunes or bars the upstream current may be able to rework sediment on the bed to form back-flow ripples, which have also been known as regressive (Jopling, 1961), counter-current (Allen, 1965), reversed-climbing (Tillman & Ellis, 1968), counter-flow (Livera & Leeder, 1981), reverse-flow (Reesink & Bridge, 2007) and return-flow ripples (Reesink & Bridge, 2009). The term back-flow ripples used here was first used by Johansson (1963). Downstream of the lee-side eddy reattachment point downstream-directed co-flow ripples can form (Fig. 1).

Relatively little has been published on back-flow ripples and bottomsets of dune and unit bar cross-stratification even though they have high preservation potential, contain features

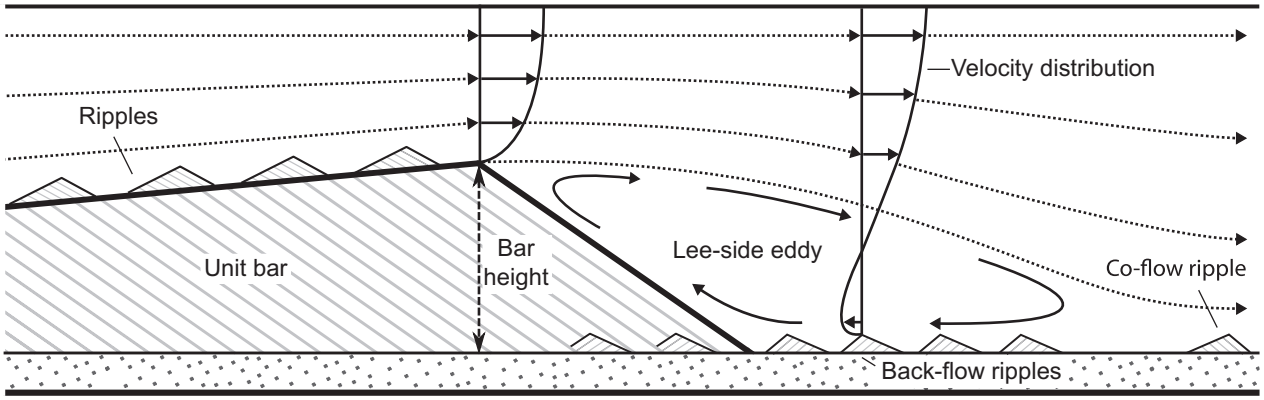

Fig. 1. Flow pattern over a large bedform with superimposed smaller bedforms, back-flow ripples and schematic representation of internal structure. The solid steel base of the channel is represented by the bold black line at the base of the schematic. The stipples represent the sand bed with structure unrelated to the ripples or the bar.

which are identifiable on the scale of cores and can act as laterally extensive partial barriers to interstitial flow.

Back-flow ripples have been identified in the lee of large ripples (e.g. Baas *et al.*, 2011), dunes (e.g. Kirk, 1983; Martinius & Van den Berg, 2011) and unit bars (e.g. Reesink & Bridge, 2011). The factors that control back-flow ripple formation depend in part on the host bedform type. Dunes form in a relatively narrow range of conditions and, if in equilibrium with the flow, their crest height is related to the water flow depth (Yalin, 1964; Allen, 1982a). Martinius & Van den Berg (2011) suggest that back-flow ripples do not form downstream of all dunes, they form in association with constructive dunes where the flow conditions allow relatively fine sediment to be deposited within the lee-side eddy; this holds true unless the flow conditions over the dunes change substantially (for example, during the falling stage of a flood). Dune three-dimensionality is also important; this influences the flow within the dune trough (Maddux *et al.*, 2003; Best, 2005; Venditti, 2007; Omidyeganeh & Piomelli, 2013) altering the characteristics of any back-flow ripples formed. Allen (1968, 1982b) noted that back-flow ripples created in the lee of long crested dunes can consist of a number of ripple fans, often bounded by spurs which extend out from the dune lee. In contrast, bars form in a wide range of conditions, may persist through varying flow conditions and their height is not directly related to flow depth. Back-flow ripples can form in a wider range of conditions (for example, velocity and flow depth above bedform) in the lee of bars than dunes. Flows along bar troughs may be more common in association with bars than dunes (Reesink & Bridge, 2011) which influences the formation and orientation of back-flow ripples.

Jopling (1961) documented back-flow ripples, created in the lee of a migrating 'delta front', during flume experiments. The maximum back-flow velocity within the lee-side eddy ranged from 16 to 33% of the mean flow velocity measured upstream of the 'delta front'. This author suggested that back-flow ripples would not form at free stream velocities $<0{\cdot}61$ m s^{-1}. Saunderson & Jopling (1980) recorded back-flow ripples in the Brampton Esker, Ontario, Canada. Based on previous flume research by Jopling these authors assumed that the back-flow must have had a mean velocity $>0{\cdot}12$ m s^{-1} to generate back-flow ripples in 'fine silty sand'. Using the Jopling (1961) relationship between the back-flow velocity and mean down-channel flow velocity, along with other methods, Saunderson & Jopling (1980) estimated a palaeocurrent velocity of $0{\cdot}65$ m s^{-1}.

Allen (1965) observed back-flow ripples in the lee of a migrating 'sand wave' within a flume and noted that, at relatively low stream velocities, ripples were generated by grain movement driven by sporadic turbulence that attained instantaneous back-flow velocities $>0{\cdot}2$ m s^{-1}. This author described ripples as subdued and 'scalelike', becoming more developed close to the 'sand wave'. Allen (1965) provided simple two-dimensional interpretations of this three-dimensional phenomena, suggesting that the sediment flux reaching the trough of the host bedform can alter the structure of the back-flow ripples. At low flow velocities a large proportion

of the sediment is deposited on the upper lee face of the host bedform and the sediment flux to the trough is small; this results in the lee face prograding discordantly over a 'pavement' of ripples (Fig. 1). At higher flow velocities more sediment can be deposited directly in the trough, resulting in a thicker bottomset layer containing ripple cross-lamination (Allen, 1965). More recent studies have linked flow deceleration to bottomset development (Reesink & Bridge, 2009, 2011), with larger decelerations over a bedform enhancing suspended sediment deposition.

Bottomset deposits are also influenced by the sediment and host bedform characteristics. Different grain sizes will alter the sediment transport dynamics over the host bedform, influencing the proportion of sediment reaching the bottomset derived from different transport mechanisms (for example, suspension and saltation). With a relatively small host bedform the bottomset could contain a significant proportion of grains saltated over the host bedform brink. As the host bedform height increases the chance of saltated grains reaching the bottomset decreases. If the host bedform features a relatively high climb angle, downstream directed co-flow ripples can be preserved within the bottomset (Boersma, 1967; Martinius & Van den Berg, 2011). In some instances the contact between the bottomset and the slip face becomes transitional with back-flow ripples interfingering with the grain flows of the host bedform lee face or becoming preserved between or at the base of the host bedform foresets.

Back-flow ripples have been observed in deposits formed in a range of modern and ancient environments, including fluvial (e.g. Basumallick, 1966; Boersma, 1967; Boersma *et al.*, 1968; Tillman & Ellis, 1968; Collinson, 1970; Gradzinski, 1970; Karcz, 1972; Van Beek & Koster, 1972; Livera & Leeder, 1981; Kirk, 1983; Hunter, 1985; Casshyap & Kumar, 1987; Smith & Edwards, 1991; Ashworth *et al.*, 2000; Reesink & Bridge, 2011), fluvioglacial (e.g. Johansson, 1963; Helm, 1971; Saunderson & Jopling, 1980), glaciolacustrine (e.g. Gustavson *et al.*, 1975; Theakstone, 1976), tidal (e.g. Nio *et al.*, 1980; De Mowbray & Visser, 1984) and shallow marine (e.g. Terwindt, 1971; Sohn *et al.*, 2003; Nielsen & Johannessen, 2009), as well as in numerous flume studies (e.g. Jopling, 1961; Johansson, 1963; Allen, 1965; Carling & Glaister, 1987; Reesink & Bridge, 2007, 2009; Baas *et al.*, 2011; Macdonald *et al.*, 2013). Ripples formed in the lee of larger bedforms have been observed to have migration directions parallel but opposed to the mean flow direction (i.e. the back-flow parallel to the stream flow; e.g. Basumallick, 1966; Boersma *et al.*, 1968), oblique to the mean flow direction (e.g. Boersma *et al.*, 1968; Van Beek & Koster, 1972; Ashworth *et al.*, 2000; Reesink & Bridge, 2011) and perpendicular to the mean flow direction (e.g. Boersma *et al.*, 1968; Collinson, 1970) buried beneath both tangential (e.g. Boersma, 1967) and angular (e.g. Tillman & Ellis, 1968) cross-strata of the host bedform.

With a very large host bedform back-flow dunes could potentially form. For example, Collinson (1968) found medium-scale cross-bedding in the lower 2 m of a 12 m thick cross-bed set with opposing palaeoflow direction in the Namurian Kinderscout Grit of Northern England. Allen (1980) suggested that back-flow dunes may explain up-slope directed cross-stratification observed in some marine deposits whilst Dasgupta & Bandyopadhyay (2008) proposed that back-flow dunes could have formed during aeolian deposition of the Late Pleistocene to Early Holocene granular carbonates of Saurashtra, India. However, these dunes could have been formed by recirculation in the horizontal plane.

Bedforms with a similar structure to back-flow ripples but a different formation mechanism have been found in tidal settings. These ripples ascend reactivation surfaces; unlike back-flow ripples, these are not created within a lee-side eddy but are formed by a transition to the subordinate-current in a bidirectional flow environment (Boersma, 1967; De Mowbray & Visser, 1984). In this article, the term *subordinate-current ripples* (cf. De Mowbray & Visser, 1984) is used to differentiate these from back-flow ripples; however, other terms also exist such as *set climbers* (Van den Berg *et al.*, 2007). Terms used for back-flow ripples have also been used to describe subordinate-current ripples formed by tidal activity (e.g. George, 2000; Kostic & Aigner, 2004; Zhang *et al.*, 2008) leading to possible confusion between ripples formed within lee-side eddies and those formed by tidal current reversal. Boersma (1967) suggested that supposed back-flow ripples found in the Folkestone Beds by Allen & Narayan (1964) were misinterpreted and were actually formed by a subordinate current. Conversely, structures attributed to tidal subordinate-current may be back-flow ripples (e.g. Abouessa *et al.*, 2012). Care should be taken when distinguishing back-flow and

subordinate-current ripples formed in tidal environments. Interfingering of foreset and bottomset is characteristic of unidirectional currents (such as in rivers), whereas subordinate-current ripples may climb high up reactivation surfaces and may contain other indicators of tidal origin such as mud drapes and periodicity (Martinius & Van den Berg, 2011, fig 3.5.1). In extreme cases sets can be constructed entirely by subordinate-current ripples (Van den Berg *et al.*, 2007).

This article aims to improve the understanding of back-flow ripples and thus the usefulness of the resulting structures for palaeoenvironmental reconstruction by answering two key questions:

1 What are the conditions required for the formation of back-flow ripples on a well-sorted sand bed?

2 Can ripple cross-lamination formed by back-flow ripples in conjunction with related cross-strata be used to improve the interpretation of palaeoenvironments?

To address these questions the formation of back-flow ripples in the lee of a large bedform (herein called a unit bar) over a range of flow conditions was examined in the University of East Anglia recirculating flume (Fig. 2A) and the resulting deposits are compared with structures found in Carboniferous sandstones at Pittenweem, Scotland.

METHODOLOGY

The flume used in these experiments has a $10 \times 1 \times 1$ m glass-walled test channel and recirculates sand and water in a closed loop, with no settling tank. In this study, the channel was horizontal and the bed consisted of well-sorted sand (D_{50} = 230 μm; Fig. 2B). Positions (x, y and z) within the channel are recorded with reference to the upstream most left-hand side of the channel floor (Fig. 2A). A unit bar was formed from a mound of sand that was modified into an asymmetrical bedform by running the flume, first at 0·06 $m^3 s^{-1}$ for 1200 sec and then at 0·10 $m^3 s^{-1}$ for 5400 sec, following a procedure similar to that used by Reesink & Bridge (2007).

Data are presented from 19 Runs (Table 1) in which back-flow ripple formation and evolution were observed directly, photographed and measured. Unit bars were formed before the start of Runs 1, 9, 17 and 19. The other runs used the bars that had been modified by the preceding run. Runs 1 to 16 were of 1800 sec duration and, at the end of each, pumping stopped and

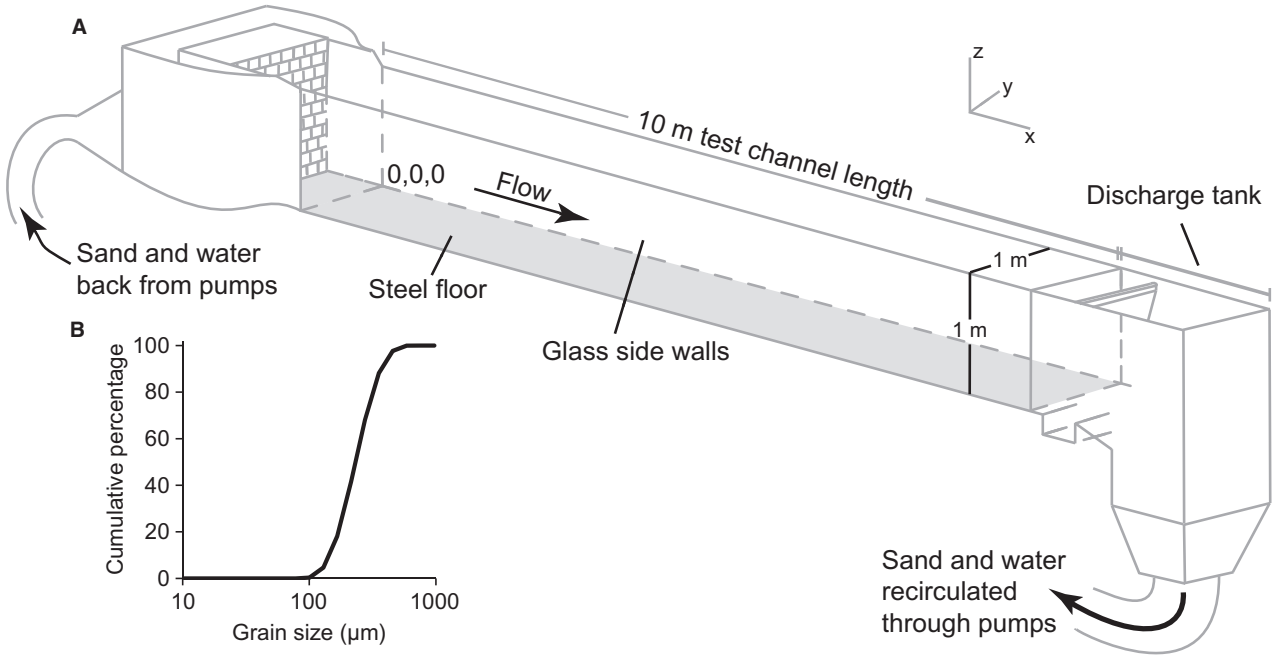

Fig. 2. (A) Schematic diagram of the flume used for the experiments (not to scale). (B) Grain-size distribution of the sand used in the flume experiments, measured using a Malvern 2000 Particle Size Analyzer (Malvern Instruments Limited, Malvern, UK).

Table 1. Experimental conditions in which back-flow ripples were observed. Run 19 consisted of one continuous 21 600 sec flume experiment which was split into six 3600 sec recording windows (denoted by subscript letter). Mean flow velocity above the unit bar brink (U_b) was calculated by dividing the discharge (which was measured using electromagnetic flow meters in the recirculation pipes) by the cross-sectional area above the brink.

Run	Duration (s)	Water level above flume base (m)	Discharge (m^3 s^{-1})	Mean flow velocity at brink U_b (m s^{-1})		Bar brink height as indicated in Fig. 1 (m)		Mean water depth over run (m)	
				Start	End	Start	End	Brink	Toe
1	1800	0·69	0·059	0·200	0·200	0·367	0·374	0·296	0·670
2	1800	0·69	0·081	0·274	0·270	0·374	0·369	0·298	0·670
3	1800	0·69	0·080	0·267	0·267	0·369	0·351	0·300	0·665
4	1800	0·69	0·101	0·337	0·321	0·351	0·340	0·308	0·660
5	1800	0·69	0·123	0·391	0·381	0·340	0·327	0·319	0·656
6	1800	0·69	0·142	0·438	0·432	0·327	0·318	0·326	0·652
7	1800	0·69	0·205	0·625	0·604	0·318	0·284	0·333	0·640
8	1800	0·69	0·263	0·777	0·703	0·284	0·175	0·256	0·592
9	1800	0·60	0·061	0·214	0·210	0·243	0·225	0·288	0·516
10	1800	0·60	0·081	0·279	0·279	0·225	0·225	0·290	0·515
11	1800	0·60	0·101	0·349	0·375	0·225	0·233	0·280	0·514
12	1800	0·60	0·121	0·447	0·372	0·233	0·188	0·298	0·511
13	1800	0·60	0·142	0·436	0·465	0·188	0·193	0·315	0·506
14	1800	0·60	0·171	0·560	0·526	0·193	0·160	0·315	0·494
15	1800	0·60	0·197	0·606	0·555	0·160	0·128	0·340	0·485
16	1800	0·60	0·234	0·659	0·650	0·128	0·125	0·358	0·485
17	10 080	0·70	0·141	0·513	0·424	0·373	0·280	0·304	0·628
18	14 940	0·70	0·141	0·424	0·389	0·280	0·233	0·348	0·608
19_a	3600	0·72	0·141	0·696	0·508	0·378	0·288	0·240	0·572
19_b	3600	0·72	0·141	0·508	0·477	0·288	0·290	0·286	0·575
19_c	3600	0·72	0·141	0·477	0·466	0·290	0·295	0·298	0·591
19_d	3600	0·72	0·141	0·466	0·466	0·295	0·288	0·302	0·593
19_e	3600	0·72	0·141	0·466	0·437	0·288	0·268	0·312	0·590
19_f	3600	0·72	0·141	0·437	0·399	0·268	0·240	0·337	0·591

all ripples in the lee of the bar were flattened before the start of the next run. In Runs 17 and 18 three velocity profiles were measured (two at $y = 0{\cdot}5$ m and one at $y = 0{\cdot}2$ m) within the lee-side eddy at a constant discharge known to form back-flow ripples using a Nortek acoustic Doppler velocimeter (ADV; Nortek AS, Rud, Norway) with a sampling volume of 1 mm and a sampling frequency of 20 Hz. The ADV probe was positioned at 0·05 m intervals above the bed and velocity was measured for 300 sec at each height. The streamwise location of the probe, x, was adjusted at each height to maintain its position relative to the lee face of the bar. Ripples in the lee of the bar were not artificially flattened between the two runs. Run 19 ran for 21 600 sec continuously at a constant discharge. The data were recorded in six individual 3600 sec intervals (denoted by subscript letters a to f; Table 1) with no artificial flattening of the bed between intervals.

The highest point of the bar (the bar crest) changed position and height rapidly as superimposed bedforms moved up to the top of the stoss side of the bar. Sometimes the crest of the bar coincided with the brink of the avalanche slip face, but at other times, when a superimposed bedform was a short distance upstream of the bar brink (as in Fig. 1), the bar crest was also some distance upstream of the bar brink. Because the crest position changed quickly but the lee face brink position changed relatively slowly, flow conditions were assessed in relation to the position of the brink. The mean flow velocity above the unit bar brink (U_b) was estimated by dividing the discharge measured electromagnetically within the flume recirculation pipes by the cross-sectional area of the flow at the unit bar brink. For this calculation it was assumed that the brink was perpendicular to the flow and that there was no flow through the sediment bed.

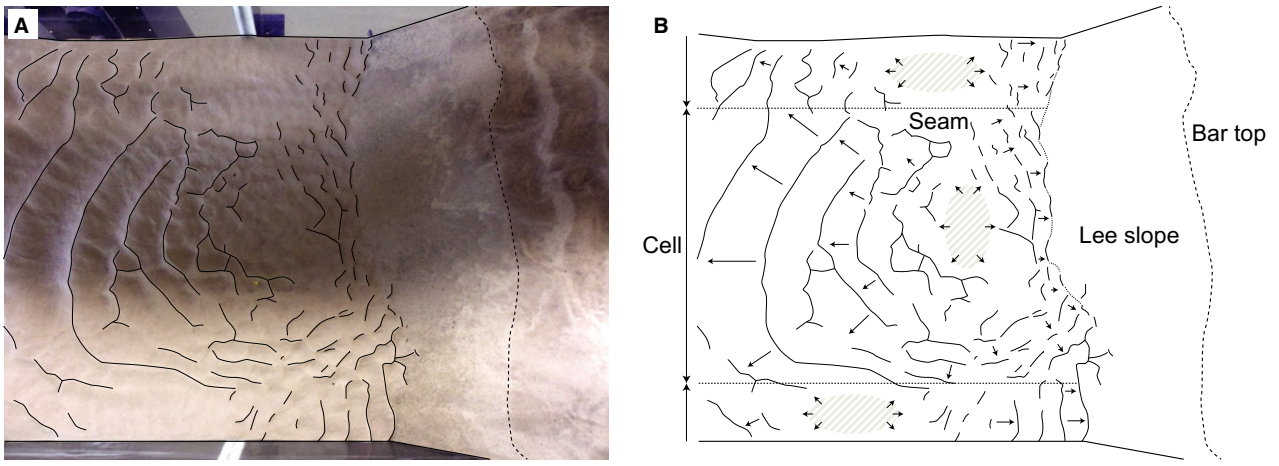

Fig. 3. (A) Ripple crests, highlighted with black lines, in the trough downstream of the unit bar formed at the end of a preliminary flume experiment (water level = 0·70 m, water depth above brink = 0·40 m, mean brink flow velocity = 0·43 m s^{-1}, mean bar height = 0·20 m). (B) Line drawing of (A) with ripple crests used to identify flow separation cells, areas where no ripples formed are highlighted with grey hatching. Arrows denote mean flow direction. Flume is 1 m wide.

RESULTS OF THE FLUME RUNS

During the runs the unit bars migrated downstream. Back-flow ripples preferentially formed near the sidewalls of the flume. The ripple crests varied from being constrained close to the side walls to extending *ca* 0·2 m out from them. Ripples that formed in the centre of the flume (away from the side wall) were smaller than those near the sides and had more variable migration directions, with their crests varying from parallel to highly oblique to the bar front (Fig. 3A). The ripple pattern generated in the trough points to the formation of multiple flow cells (Fig. 3B; cf. Allen, 1968). In the runs where back-flow ripples occurred, the number formed varied from one to trains of up to eleven and they were always present at the toe of the lee face of the unit bar. The ripple trains extended downstream <0·7 m from the lee face toe.

Back-flow ripples formed at U_b between 0·27 m and 0·78 m s^{-1}, the upper end of this range was the highest velocity tested. The height of the back-flow ripples, measured from the ripple trough to the ripple crest, increased with increasing U_b and also showed a very weak dependence on unit bar height within the range investigated (Fig. 4A and B). The variation in the height of individual back-flow ripples generally increased with increasing U_b (Fig. 4A; Tables 1 and 2).

The difference in depth between the brink and trough is an important control on flow separation. The height of unit bars relative to flow depth varies from very small (low bars in deep flow) to near unity (bar height approaching the full flow depth) resulting in significant differences in flow deceleration over bars. The ratio between the water depth over the brink and trough averaged over each run varied from 0·42 to 0·74 and showed no relationship (R^2 = 0·02) to back-flow ripple height under the tested conditions. However, ripple height had a relatively strong dependence on flow deceleration over the bar, with greater deceleration associated with larger ripples (Fig. 4C). Ripple height was also related to the Van den Berg & Van Gelder (1993) modified mobility parameter θ' (Fig. 4D). Over Runs 1 to 19 back-flow ripples were observed forming mostly outside the conditions suggested for dune-related bottomset development (Fig. 5; Martinius & Van den Berg, 2011). Three categories of ripple were identified: *incipient* (Fig. 6), *conventional* (Fig. 7) and *transient* (Fig. 8) back-flow ripples.

Incipient back-flow ripples

Incipient back-flow ripples formed in the trough at U_b ranging from 0·27 to 0·34 m s^{-1} and 0·35 to 0·38 m s^{-1} in runs with a water surface 0·69 m and 0·60 m above the flume base, respectively (Tables 1 and 2). In Runs 4 and 11 some of the incipient back-flow ripples grew into conventional back-flow ripples by the end of the run. Incipient back-flow ripples ranged in height

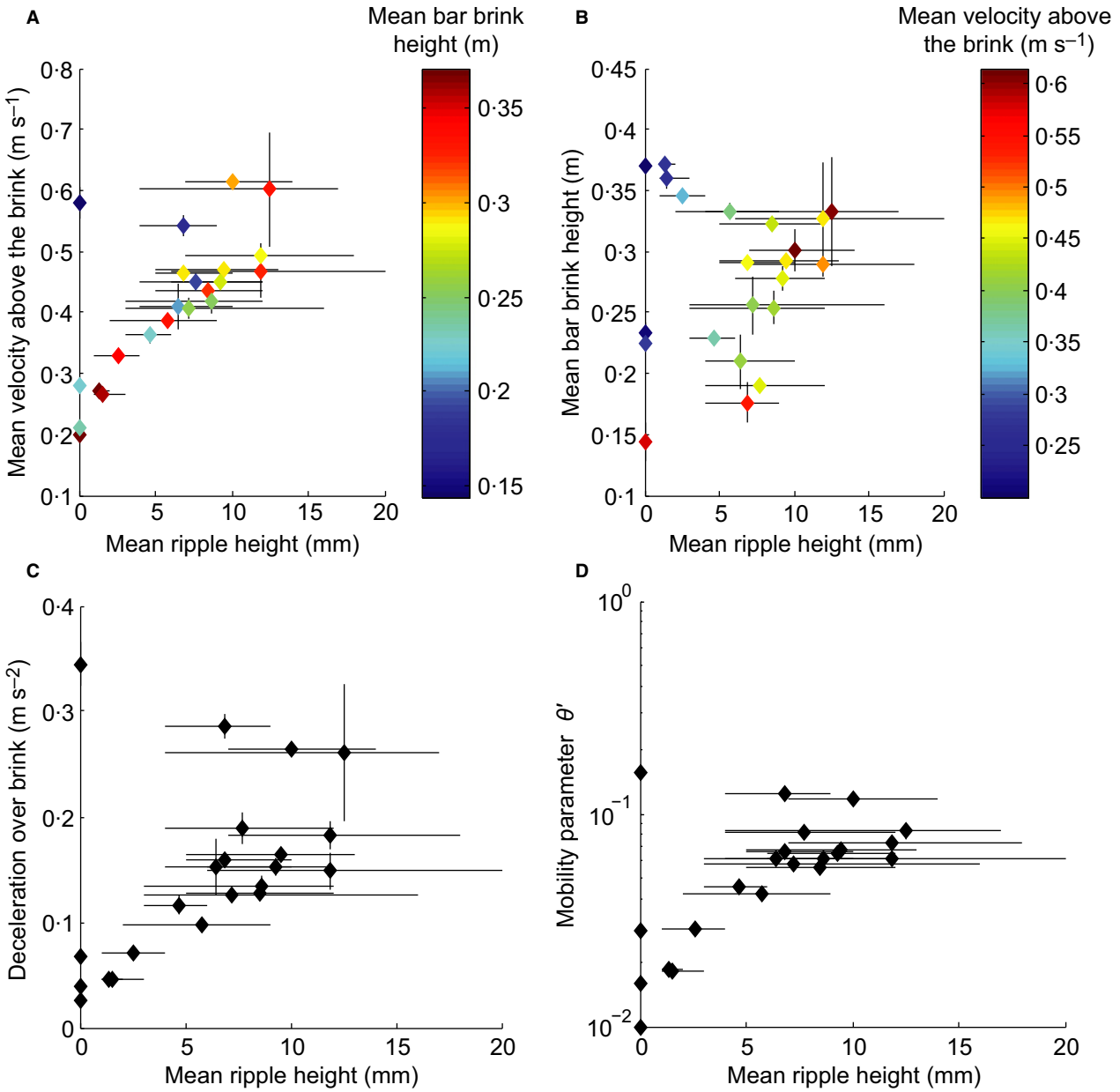

Fig. 4. (A) Mean height of back-flow ripples (incipient and conventional) against the mean velocity above the brink of the bar U_b. (B) Mean ripple height against mean unit bar brink height (see Fig. 1). (C) Mean ripple height against the deceleration of the flow between the brink and trough. (D) Mean ripple height against the modified mobility parameter (cf. Van den Berg & Van Gelder, 1993). Bars denote the data range. To calculate θ' it was assumed that the density of the quartz rich sand was 2650 kg m^{-3}. This calculation also required depth averaged flow velocity to be determined in relation to the mean water depth between the bar brink and trough. Side wall effects were corrected for by multiplying this velocity by an average correction factor. This correction factor was calculated from velocity profiles collected with an ultrasonic Doppler velocity profiler over twelve additional flume runs. Over these runs the average correction factor was 1·06 (minimum: 1·04, maximum: 1·07) and showed no dependence to the width to depth ratio.

from 1 to 4 mm, featured straight to sinuous crests and formed in the fine sand deposited in the trough. Incipient back-flow ripples featured a long shallow-dipping stoss and a short high-angle lee slope (Fig. 6A). Height : length ratios of these ripples were low (0·01 to 0·05). The ripples were easily removed by grain flows on the unit bar lee slope and no evidence of them was

Table 2. Minimum, maximum and mean heights for up to ten back-flow ripples (five from each side of the flume closest to the unit bar toe) recorded at the end of each run. In some runs less than ten ripples were present, in these cases the mean is calculated from the number of ripples present. Only an approximate height is given for transient back-flow ripples as their short existence period made them difficult to measure. Runs 15 and 16 featured conventional back-flow ripples at the start of the run transitioning to no ripples and transient back-flow ripples, respectively, by the end. For Run 15 these changes resulted from the breakdown of the lee-side eddy induced by a large superimposed bedform.

Run	Back-flow ripple height (mm)			Dominant ripple type
	Min	Max	Mean	
1	0	0	0·0	None
2	1	2	1·3	Incipient
3	1	3	1·5	Incipient
4	1	4	2·6	Incipient, Conventional
5	2	9	5·8	Conventional
6	5	12	8·5	Conventional
7	7	14	10·0	Conventional
8	*ca* 4	*ca* 10	–	Transient
9	0	0	0·0	None
10	0	0	0·0	None
11	3	6	4·7	Incipient, Conventional
12	4	10	6·4	Conventional
13	4	12	7·7	Conventional
14	4	9	6·9	Conventional
15	0	0	0·0	Conventional, None
16	*ca* 4	*ca* 10	–	Conventional, Transient
17	6	20	11·9	Conventional
18	3	16	7·2	Conventional
19_a	4	17	12·5	Conventional
19_b	7	18	11·9	Conventional
19_c	5	13	9·5	Conventional
19_d	5	10	6·8	Conventional
19_e	6	12	9·3	Conventional
19_f	3	12	8·6	Conventional

observed in the preserved deposits. Occasionally at higher U_b incipient back-flow ripples formed on the unit bar lee slope while conventional back-flow ripples formed in the trough (Fig. 6B).

Conventional back-flow ripples

Conventional back-flow ripples (so called because they look like those described by Jopling, 1961; Johansson, 1963; Basumallick,

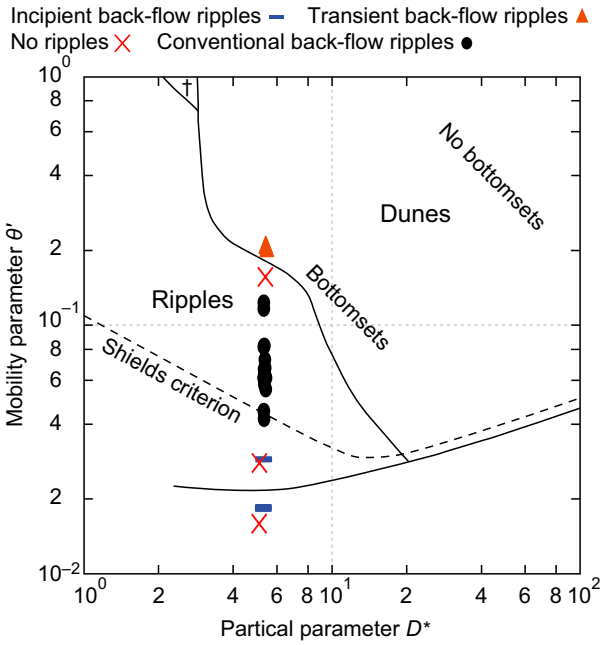

Fig. 5. Back-flow ripple presence and type plotted on a bedform stability diagram from Van den Berg & Van Gelder (1993). The areas with favourable and unfavourable conditions for dune-related bottomset development suggested by Martinius & Van den Berg (2011) are also indicated. Upper plane bed region is represented with a †.

1966) formed in the unit bar trough at U_b of 0·32 to 0·7 m s^{-1} (Tables 1 and 2). Their height ranged from 3 to 20 mm and their height : length ratios (0·05 to 0·25) were greater than incipient back-flow ripples. These ripples had straight to sinuous crests, moved towards the lee face of the bar (Fig. 7A) and occasionally travelled tens of millimetres up it. As the unit bar advanced, the ripples were buried beneath grain flows (Fig. 7B), creating structures like those observed in the rock record (Fig. 7C to E).

Runs 17 and 18 resulted in the preservation of conventional back-flow ripples within the unit bar deposits. Their preserved structure was predominantly controlled by the height that migrating ripples reached up the lee slope prior to being buried by grain flows. If no migration occurred prior to burial the ripples were confined to the bottomset, sometimes showing a symmetrical structure due to deformation caused by sand avalanching down from the lee of the unit bar (Fig. 7B). When back-flow ripples migrated up the unit bar lee slope, a wedge shaped ripple was preserved and the back-flow ripples would sometimes interfinger with the

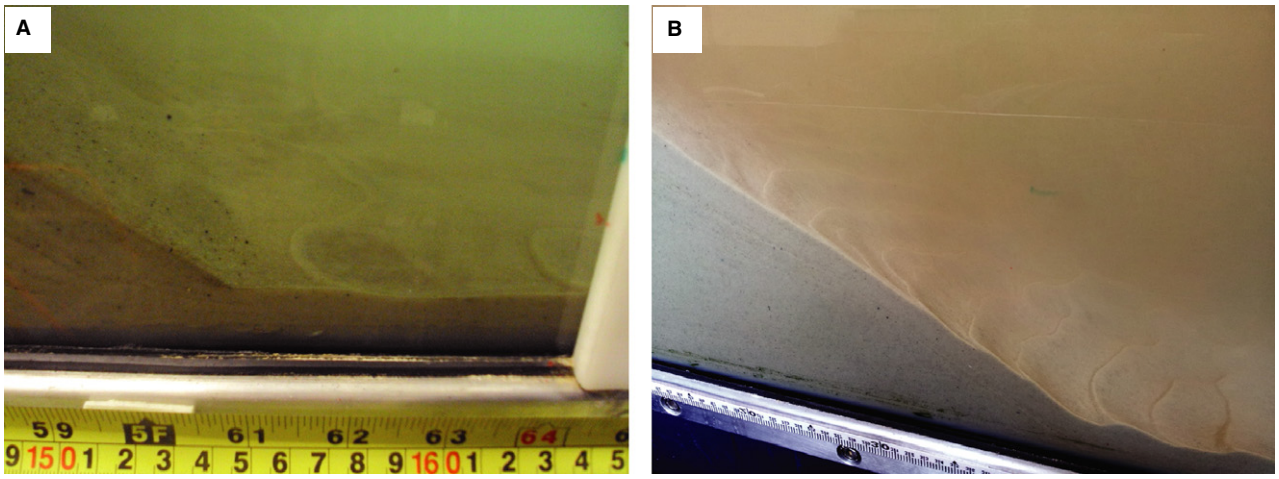

Fig. 6. Incipient back-flow ripples; (A) in the trough with no ripples forming on the lee face of the unit bar, and (B) on the lee slope of the unit bar with larger conventional back-flow ripples beginning to develop in the trough (the three ripples on the right side of the photograph).

unit bar foresets (Fig. 7F) extending up to 70 mm up slope (*ca* 11% of the bar lee face) from the base of the foreset. Where this occurred, the base of the unit bar foreset curved tangentially towards the ripples.

Transient back-flow ripples

Transient back-flow ripples sporadically formed in the trough and on the lee slope of the unit bar when $U_b >$ 0·65 m s^{-1} (Tables 1 and 2; Fig. 8A and B). Due to the turbid nature of the flow, observations of these ripples were limited towards the side walls; they formed rapidly, taking only a few seconds to reach heights of *ca* 4 to 10 mm, but within a few seconds were washed out by a change in near-bed flow or through entrainment into grain flows on the bar lee face. During their brief existence these ripples rapidly migrated hundreds of millimetres towards the bar lee slope; their occurrence coincided with the transition from angular to tangential lee face laminae downlap. The migration of transient back-flow ripples up the bar lee face contributed to an observed decrease in grain size in the unit bar foresets; this was due to the remobilization of relatively finer sand, deposited from suspension in the bar trough, up the bar lee face. This effect, combined with ripple scouring, also caused increased grain-size heterogeneity within cross-stratum but decreased the grain-size variation between cross-strata. Transient back-flow ripples were often incorporated into grain flows on the unit bar lee face or were destabilized by a change in the lee-side eddy flow conditions and generated grain flows. Because of their rapid washing out, these ripples were infrequently preserved within the deposit as slight undulations on bar foreset cross-stratum (Fig. 8C).

Velocity profiles in the lee of the bar

Velocity data within and above the lee-side eddy were collected in Runs 17 and 18, while conventional back-flow ripples formed in the lee of the unit bar. The unit bar prograded 0·44 m in Run 17 and 0·29 m in Run 18. The ripples were progressively buried under grain flows as the bar moved downstream.

Three velocity profiles were constructed; two at the bar toe at y = 0·5 m and y = 0·2 m and one 0·1 m downstream of the toe at y = 0·5 m (Fig. 9A to C). At all three locations time averaged downchannel velocities ($\bar{u}$) near the water surface were *ca* 0·4 m s^{-1}, further down the water column much lower velocities or reversed flow was recorded. Within the lee-side eddy the magnitude of the back-flow velocity was higher closer to the sidewall (Fig. 9B). At y = 0·5 m $\bar{u}$ near the unit bar toe was close to 0 m s^{-1} (Fig. 9A) but, despite this, small ripples still formed.

Within the lee-side eddy 0·1 m above the bed the downchannel velocity component (u) ranged from −0·49 to 0·54 m s^{-1} [standard deviations (σ) 0·075 m s^{-1} to 0·103 m s^{-1}; Fig. 10A, C and E]. The mean flow direction at the flume centreline within the lee-side eddy had a significant

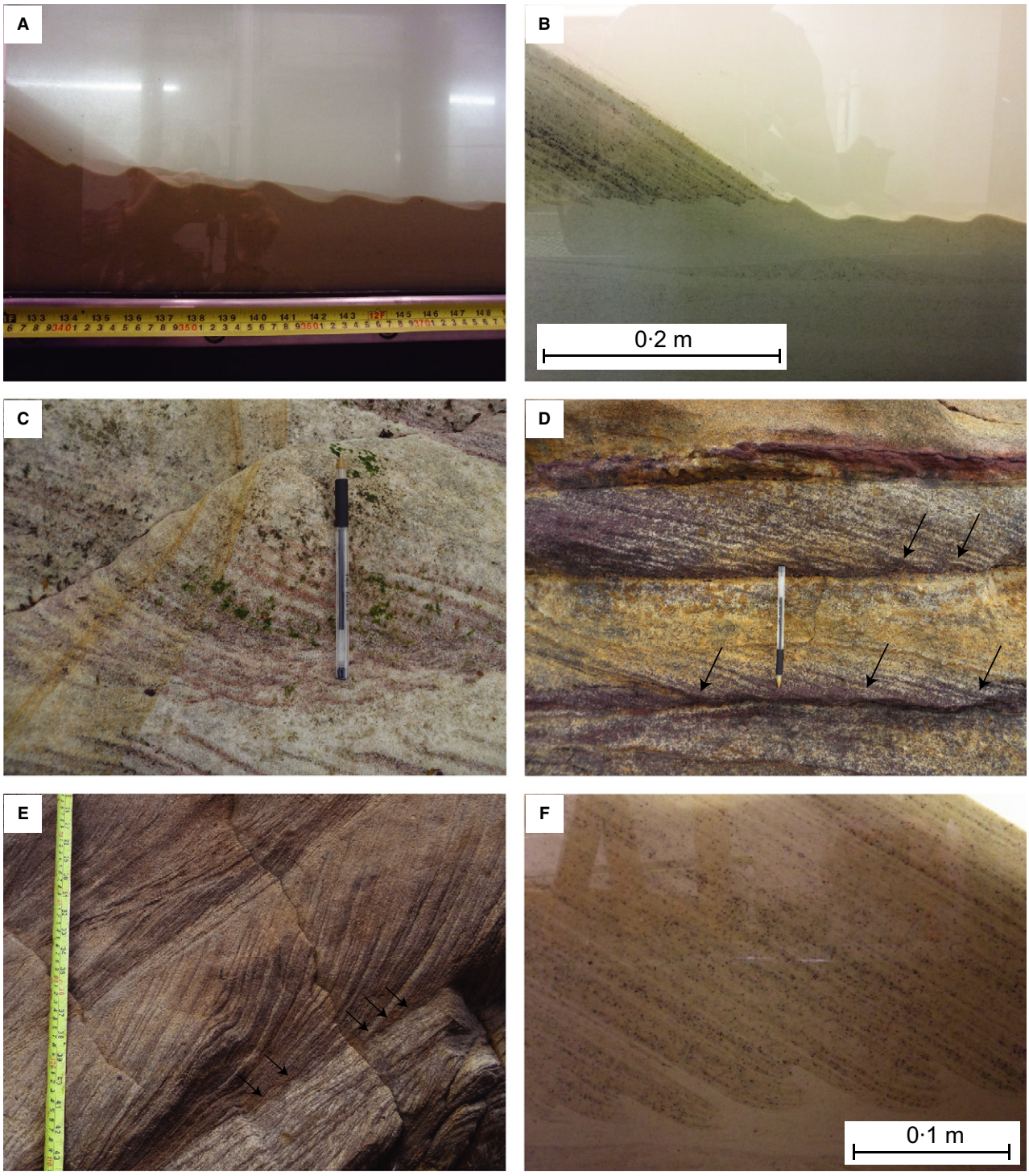

Fig. 7. Conventional back-flow ripples; (A) in the flume; (B) in the flume being buried by unit bar lee face grain flows; (C) to (E) preserved within Carboniferous cross-stratified sandstone at Pittenweem, Scotland; (F) in the flume causing interfingering of ripple cross-lamination and bar foreset laminae. Ripples are indicated by arrows in (D) and (E). The pen in (C) and (D) is 0·14 m long.

lateral component and above the toe there was also a considerable vertical component towards the bed (Fig. 10A and E). Variation in u was greater at $y = 0{\cdot}5$ m (Fig. 10A and E) and decreased close to the side walls (Fig. 10C). At the flume centreline ($y = 0{\cdot}5$ m) u was positive

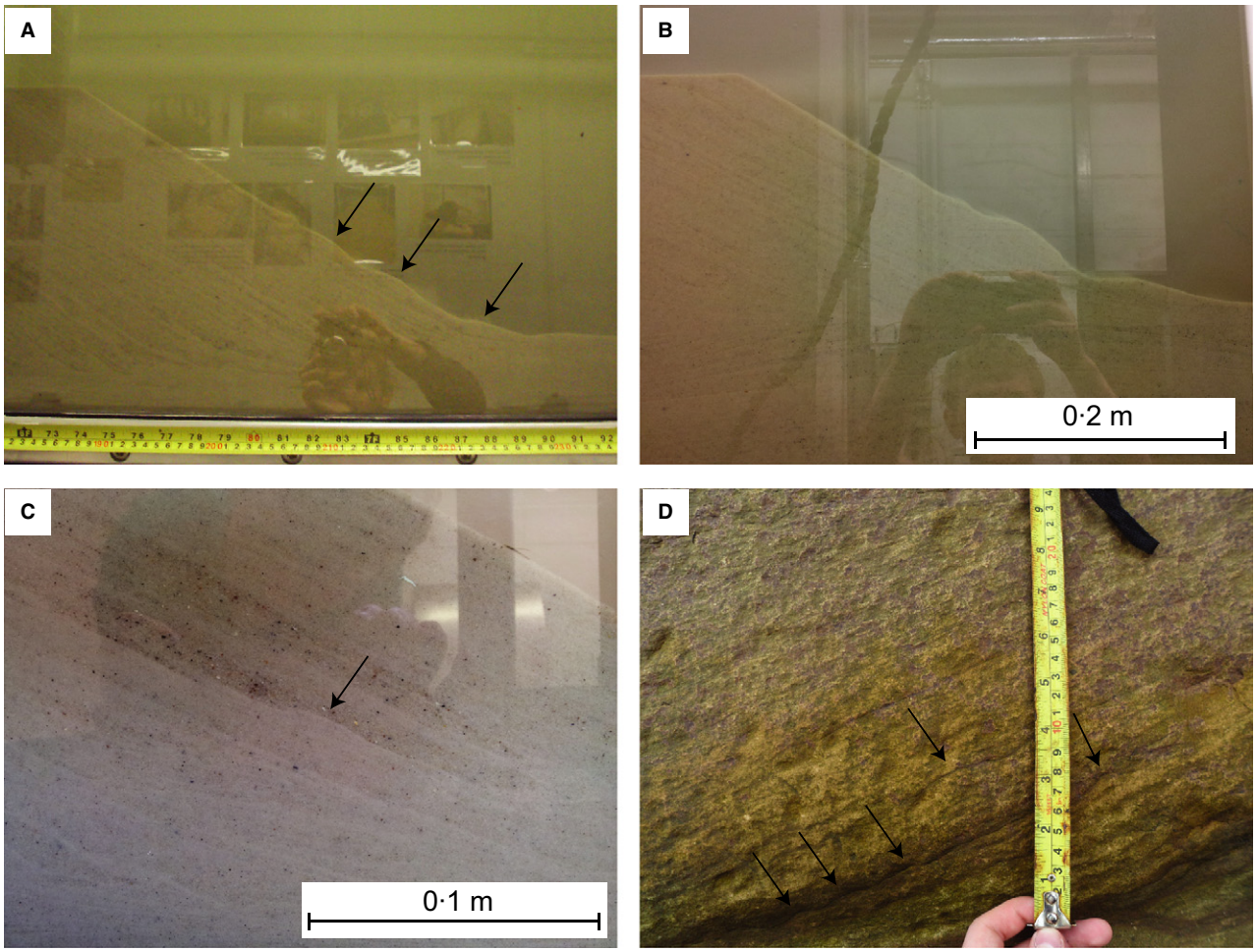

Fig. 8. Transient back-flow ripples; (A) and (B) in the flume; (C) buried within unit bar lee face grain flows; (D) preserved within Carboniferous trough cross-stratified sandstone at Pittenweem, Scotland. Ripples are identified by arrows in (A), (C) and (D).

for short periods (Fig. 10A and E) suggesting periodic weakening or breakdown of the flow separation cell. Wavelet analysis of the time series data has been applied using the method described in Torrence & Compo (1998) and Liu *et al.* (2007). This technique allows for the decomposition of the velocity time series identifying periodicity and how this periodicity varies with time (Fig. 11). Peaks can be seen between periods of 4 to 32 sec (Fig. 11A, C and E). Smaller peaks are also present at periods of >32 sec; however, for these longer period velocity fluctuations the recording window was too short to adequately quantify them using wavelet analysis.

Over the lee-side eddy 0·5 m above the bed u ranged from −0·15 to 0·75 m s^{-1} (σ 0·065 m s^{-1} to 0·077 m s^{-1}; Fig. 10B, D and F). Relative to u the flow had minimal lateral and vertical velocity components and lacked the long period velocity fluctuations found close to the bed (Figs 10 and 11). Instead higher frequency turbulence with periods between 0·5 to 4 sec was more predominant (Fig. 11). The magnitude of u fluctuations were significantly lower than in recordings taken at y = 0·5 m close to the bed.

DISCUSSION

Controls of back-flow ripple formation

Yalin (1985) stated that ripple geometry is controlled by five characteristic parameters: fluid density, kinematic viscosity, shear velocity, grain size and specific weight of the grains in the fluid. Back-flow ripples are controlled by sediment availability and the flow within the

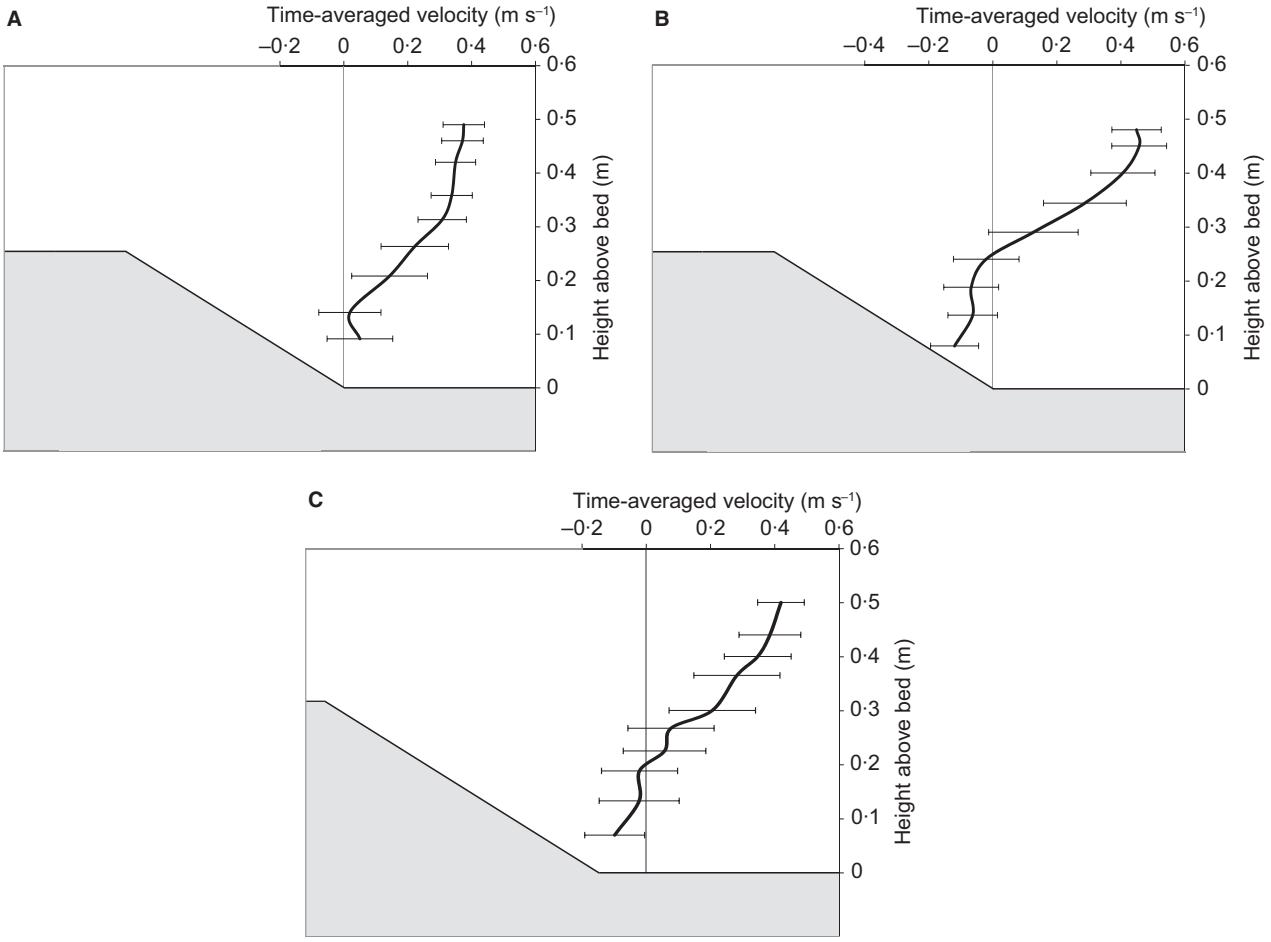

Fig. 9. Profiles of mean velocity (data recorded over 300 sec at 20 Hz for each measurement) recorded downstream of the unit bar; (A) at y = 0·5 m at the bar toe; (B) at y = 0·2 m at the bar toe; (C) 0·1 m downstream of (A). Bars denote the standard deviation.

separation eddy in the lee of the host bedform. The lee-side eddy length is controlled by the host bedform height and the brink angle (Schatz & Herrmann, 2006; Paarlberg *et al.*, 2007). Host bedform height also influences the velocity gradient within the lee-side eddy, and thus shear velocity. The velocity above the crest of the host bedform (U_b herein) controls the velocity within the separation eddy and thus influences back-flow ripple size and morphology.

Jopling (1961) suggested that a minimum stream velocity of 0·61 m s^{-1} was required to form back-flow ripples, but did not indicate how this would vary with changes in the host bedform or sediment characteristics. In Runs 1 to 19 back-flow ripples formed when U_b >0·27 m s^{-1}, and conventional back-flow ripples formed at U_b of 0·32 to 0·7 m s^{-1}. Allowing for some dissimilarity in the way velocities were assessed, this demonstrates that back-flow ripples can form at much lower velocities than Jopling (1961) stated and suggests that some published estimates of palaeocurrent velocity deduced from back-flow ripples (e.g. Saunderson & Jopling, 1980) could be overestimated.

If the entrainment velocity for 230 μm sand is 0·274 m s^{-1} (Miller *et al.*, 1977), and the flume sand D_{50} = 230 μm, it might be a surprise that back-flow ripples form at velocities significantly lower than this. Part of the explanation is the dynamic size sorting that operates over the bar-form such that the sand deposited in the trough and reworked by the return flow, has a finer grain size than the bulk sand in the flume.

Mean flow direction within lee-side eddies was found to be oblique to the bar lee face, with this being more pronounced at the flume centreline (Fig. 10); this explains the more oblique orientation of some back-flow ripple crest lines close to the flume centreline (Fig. 3). In the

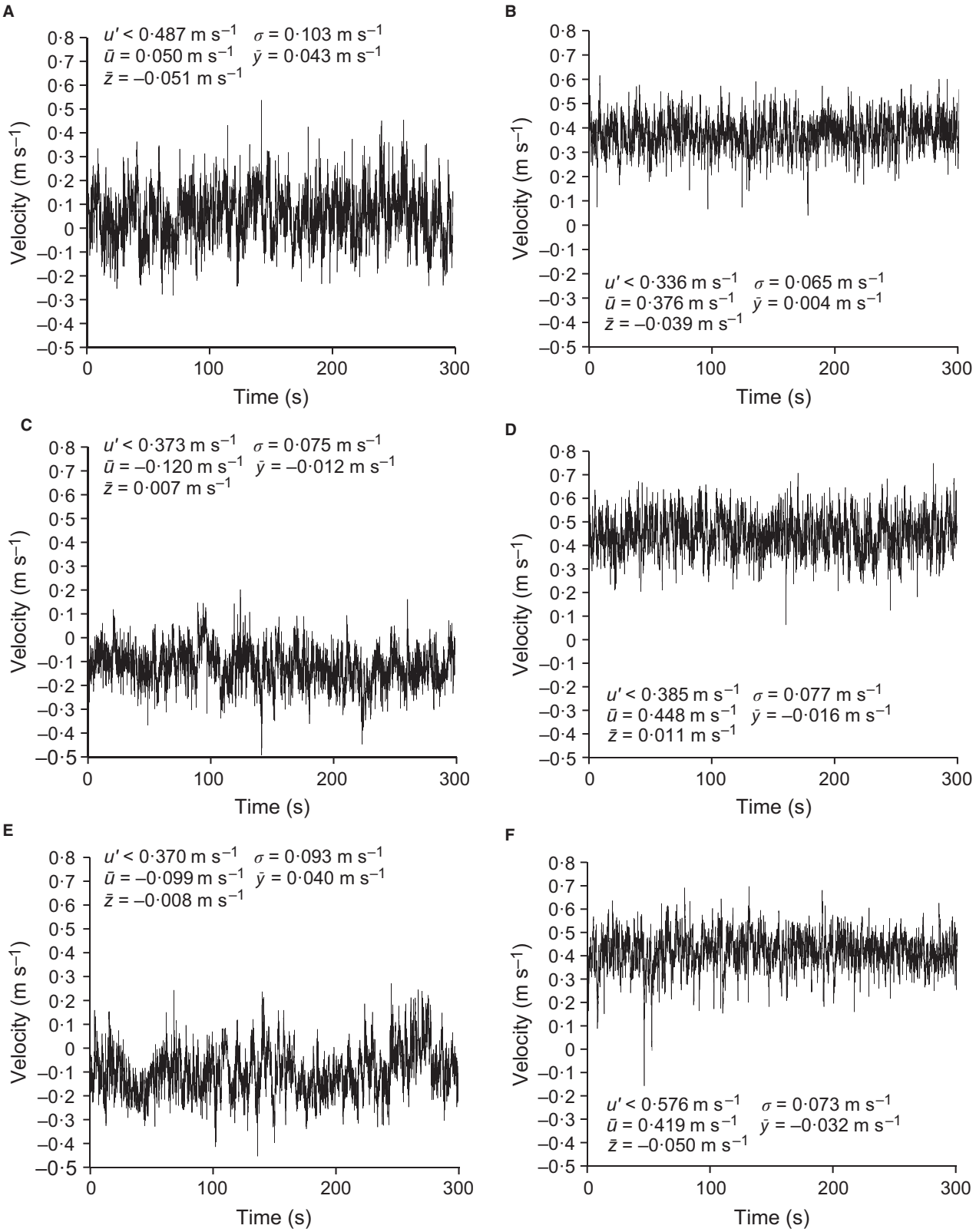

Fig. 10. Velocity time series recorded; (A) at $y = 0{\cdot}5$ m, 0·09 m above the unit bar toe; (B) at $y = 0{\cdot}5$ m, 0·49 m above the unit bar toe; (C) at $y = 0{\cdot}2$ m, 0·08 m above the unit bar toe; (D) at $y = 0{\cdot}2$ m, 0·48 m above the unit bar toe; (E) at $y = 0{\cdot}5$ m, 0·07 m above the bed, 0·1 m downstream of the unit bar toe; (F) at $y = 0{\cdot}5$ m, 0·5 m above the bed, 0·1 m downstream of the unit bar toe.

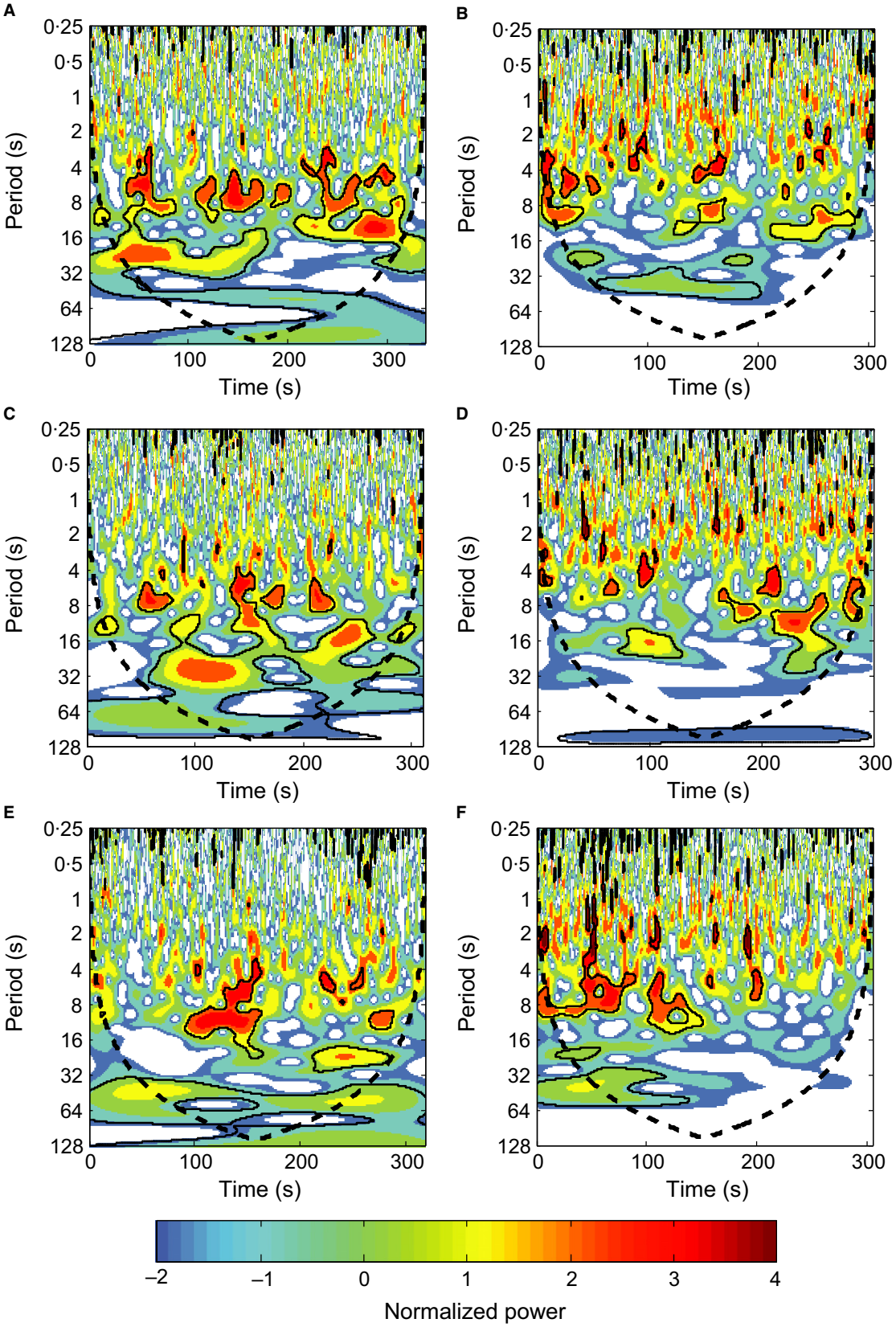

Fig. 11. Wavelet power spectrum (using the Morlet wavelet) of the velocity time series recorded at (A) at $y = 0{\cdot}5$ m, 0·09 m above the unit bar toe; (B) at $y = 0{\cdot}5$ m, 0·49 m above the unit bar toe; (C) at $y = 0{\cdot}2$ m, 0·08 m above the unit bar toe; (D) at $y = 0{\cdot}2$ m, 0·48 m above the unit bar toe; (E) at $y = 0{\cdot}5$ m, 0·07 m above the bed, 0·1 m downstream of the unit bar toe; (F) at $y = 0{\cdot}5$ m, 0·5 m above the bed, 0·1 m downstream of the unit bar toe. Contours are normalized power (normalized by variance) in logarithm (base 2) and have been rectified for bias (cf. Liu *et al.*, 2007). A solid black line encloses regions of greater than 95% confidence for a red-noise process. The curved dashed line indicates the cone of influence. Below this, edge effects can influence the power distribution. Due to this, additional measurements beyond the 300 sec recording window were also used when available. A detailed explanation of the method used can be found in Torrence & Compo (1998) and Liu *et al.* (2007).

flume, secondary currents are generated by turbulence anisotropy induced by its non-circular cross-sectional morphology (Nezu & Nakagawa, 1993) with the width to depth ratio of the flow being an important control. In these experiments width to depth ratios varied from 4·2 to 2·8 above the brink and 2·0 to 1·5 above the trough. At width to depth ratios of <5 secondary currents generated at the side walls can influence the flow (Nezu & Nakagawa, 1993) and at greater width to depth ratios secondary currents can be induced in the centre of the flow by sediment ridges on the bed (Nezu *et al.*, 1985). Secondary currents induced by the width to depth ratio could influence the orientation of back-flow ripples generated in the bar trough. This effect may be less pronounced when the bar shows significant three dimensionality (Allen, 1968, 1982b). Secondary currents induced by both the width to depth ratio and bar three dimensionality probably influenced the distribution of ripples in these flume experiments (Fig. 3). Back-flow ripples were generally larger within 0·2 m of the flume side wall, which was not observed in previous flume studies by Reesink & Bridge (2007) and Johansson (1963); this is due to differences in the secondary circulation patterns probably induced by different width to depth ratios. Unit bar experiments by Reesink & Bridge (2007) generally featured higher width to depth ratios, ranging from 10 to 4 above the brink and 3·0 to 1·7 above the trough. This finding raises questions on how applicable the relationships between back-flow ripples, flow and sediment characteristics found in flume experiments are to natural environments where no side wall would be influencing the flow. However, secondary flow cells exist in river systems and are an intrinsic part of the flow. Flow patterns within troughs downstream of bars are likely to be equally if not more three-dimensional, influenced by channel bends, tributaries, channel banks and obstacles, as well as obliquely orientated and three-dimensional bar fronts.

Reesink *et al.* (2014) suggested that oblique flows are important for the formation of back-flow ripples that climb onto the lee slope of the host bedform; Fig. 3 somewhat supports this theory with back-flow ripples that are oblique to the bar front migrating further up the lee slope. Incipient back-flow ripples forming directly on the bar lee face had variable crest line orientations often oblique to the bar front. However, climbing conventional back-flow ripples were observed forming close to the sidewalls where flow featured less obliquity (Fig. 10C). Back-flow ripple crest line orientations near the side walls were often nearly parallel to the bar front, suggesting little influence from oblique flow. This may suggest that, while the lack of oblique flow does not preclude the formation of climbing back-flow ripples, oblique currents may increase the chances of climbing back-flow bedforms.

Previous experiments suggested that back-flow velocity must exceed $0{\cdot}12$ m s^{-1} before back-flow ripples will form in 'fine silty sand' (Saunderson & Jopling, 1980, and references therein). However, in Runs 17 and 18 the magnitude of $\bar{u}$ recorded above conventional back-flow ripples within the lee-side eddy was often less than $0{\cdot}12$ m s^{-1} (Figs 9, 10A, 10C and 10E). Back-flow ripple development can be explained by $\bar{u}$ measured at the flume centreline only being a component of an oblique flow, and also the variable velocity within the unit bar lee resulting from wake flapping and vortex shedding from the separation zone. Wavelet analysis of the u time series close to the bed in Runs 17 and 18 identifies a number of strong peaks spread across a wide range of periods (Fig. 11). Turbulence periodicities have been estimated (Table 3) using scale relations proposed by Simpson (1989). Wavelet analysis identifies large peaks in normalized power between 4 and 8 sec for both Run 17 (Fig. 11E) and Run 18 (Fig. 11A and C), this is close to the estimated vortex shedding periods (Table 3). Slightly smaller peaks in normalized power can be seen at 32 to 64 sec in

Table 3. Predicted turbulence periodicities based on a range of estimated mean flow separation lengths. Estimates of periodicities are derived from the scale relations proposed by Simpson (1989). For vortex shedding $P_v \approx x_r/0{\cdot}7U_b$ where P_v is the periodicity of vortex shedding and x_r is the flow separation length. In this case U_b is multiplied by 0·7. Simpson (1989) suggests a range for this value from 0·6 to 0·8, for this equation Kostaschuk (2000) and Shugar *et al.* (2010) use 0·8 whilst Hardy *et al.* (2009) use 0·6. For wake flapping $P_w > x_r/0{\cdot}1U_b$ where P_w is the periodicity of wake flapping. The estimates are derived using a bar height of 0·327 m and 0·257 m and U_b of 0·47 m s^{-1} and 0·41 m s^{-1} in Runs 17 and 18, respectively.

	Flow separation length estimates (m)			Periodicity (s)			
				Vortex shedding		Wake flapping	
Run	Bennett & Best (1995)	Carling *et al.* (2000)	Paarlberg *et al.* (2007)	Min	Max	Min	Max
17	1·39	2·71	1·69	4·2	8·2	29·6	57·7
18	1·09	2·13	1·33	3·8	7·4	26·6	52·0

Run 17 (Fig. 11E) and 16 to 32 sec in Run 18 (Fig. 11A and C) which is close to the estimates of wake flapping periodicity (Table 3). Kostaschuk (2000) observed similar velocity patterns in data collected downstream of a dune in Canoe Pass, Canada.

In addition to wake flapping and vortex shedding, the lee-side eddy changes with the arrival of superimposed bedforms at the bar crest. This causes velocity fluctuations with a period influenced by the migration rate of the superimposed bedforms and explains some of the long period peaks (>64 sec) recorded close to the bed (Fig. 11). Vortex shedding, wake flapping and superimposed bedforms all result in packets of flow near the bed in the bar lee with much greater velocity magnitude than $\bar{u}$.

In settings where the mean return flow is not fast enough to generate ripples, fast flow packets from any of the three mechanisms described above may induce back-flow ripple formation if the minimum velocity required for ripple generation is exceeded for long enough. Within the lee-side eddy the mean back-flow velocity (labelled V_1 on Fig. 12A) may not be fast enough to initiate grain movement, but high velocity packets from eddies may allow sporadic grain movement and incipient back-flow ripple development (Fig. 12A). With an increase in the size of the lee-side eddy induced by wake flapping the mean back-flow velocity (labelled V_2 on Fig. 12B) is strengthened compared to its previous state ($V_2 > V_1$; cf. Allen, 1968; Simpson, 1989). With more frequent or longer duration high velocity packets more grain movement on the bed results in the development of conventional back-flow ripples (Fig. 12B). In settings where the mean back-flow velocity (labelled V_3 on Fig. 12C) is fast enough for transient back-flow ripple formation, slower flow packages may generate transient back-flow ripples that are periodically washed out by faster flow packages (Fig. 12C). With an increase in the size of the lee-side eddy induced by wake flapping the mean back-flow velocity increases (labelled V_4 on Fig. 12D, $V_4 > V_3$). Conditions may no longer favour the generation of back-flow ripples (Fig. 12D).

Superimposed bedforms can alter flow separation, turbulence and geometry. Fernandez *et al.* (2006) observed higher levels of turbulence intensity, Reynolds stresses and turbulent kinetic energy downstream of a fixed bedform when a fixed superimposed ripple was located 0·03 m (33% of the wavelength of the superimposed ripple) from the host bedform crest. These authors found that the lee-side flow structure was altered by the interaction of the shear layers produced from the adjacent flow separation zones of the host and superimposed bedform both of which periodically merged forming a larger unified flow separation zone leading to increased turbulence production. However, it is unlikely that the large effect observed in these experiments would be found in natural fluvial systems because the large superimposed bedform (66% of the host bedform height) would generate a reactivation surface (McCabe & Jones, 1977). Although a similar effect, albeit probably lower magnitude, is possible if the superimposed bedform height is <25% of the host bedform height precluding reactivation surface formation (Reesink & Bridge, 2009). Relatively small superimposed bedforms could lead to more rapid conventional back-flow ripple development during periodic merging of the flow

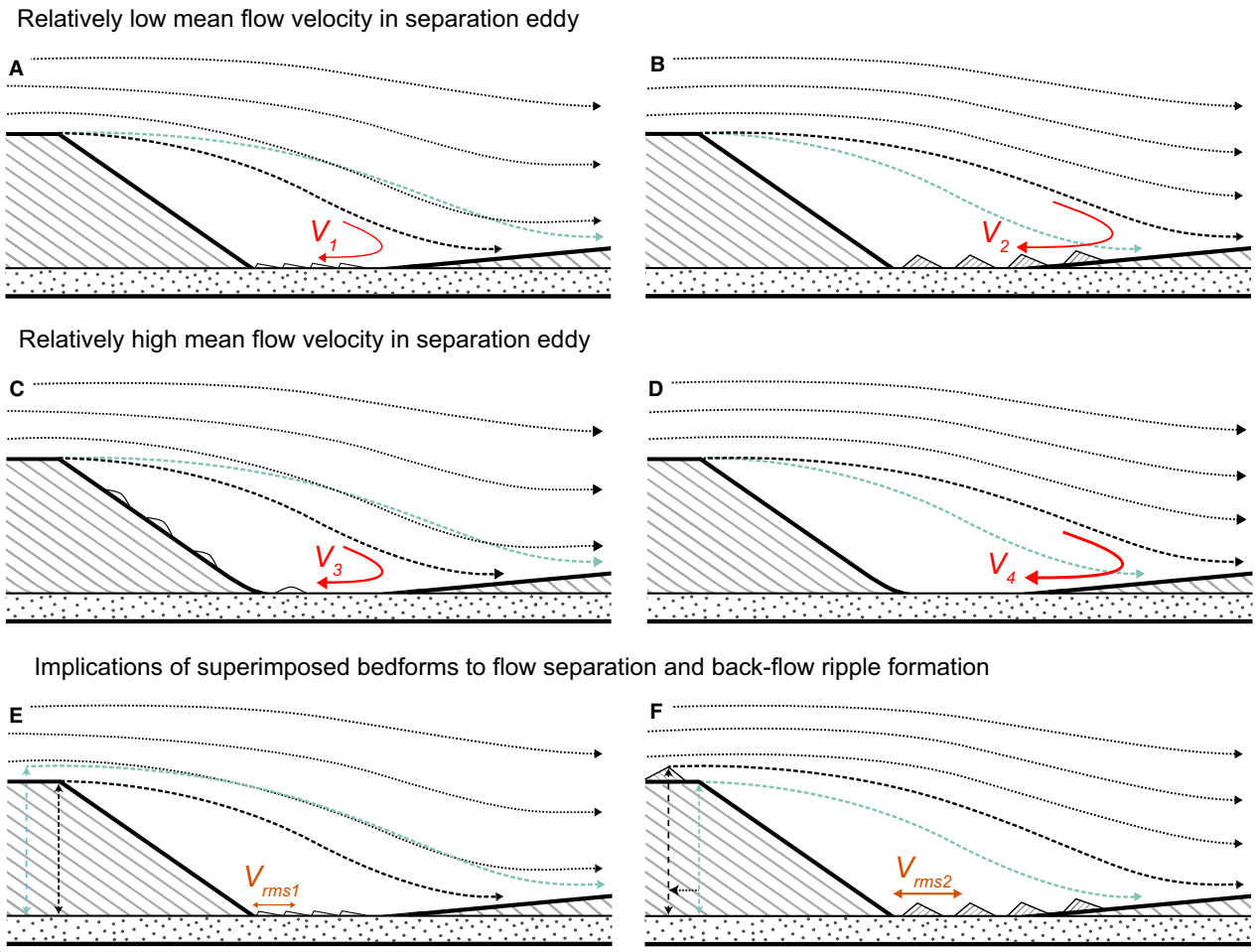

Fig. 12. Ripple formation with different lee-separation eddy flow under low (A), (B), (E) and (F), and high (C) and (D) mean velocity conditions. The position of the flow separation streamline changes between the extremes represented by the black and blue dashed lines.

separation zones (Fig. 12E and F) by allowing more grain movement induced by either longer duration, more frequent or higher magnitude velocity packets (represented on Fig. 12E and F by the root mean square back-flow velocity, V_{rms}, where $V_{rms2} > V_{rms1}$). Best *et al.* (2013) found that for relatively large superimposed bedforms which generate reactivation surfaces, the migration of the superimposed bedform to the brink decreases the size of the lee-side eddy of the host bedform. This decrease in lee-side eddy size could also occur with a relatively small superimposed bedform if its lee-side eddy erodes the brink point of the host bedform, as the angle between the brink and crest (which could potentially be the crest of the superimposed bedform) can control the size of the flow separation zone (Paarlberg *et al.*, 2007). This suggests that the time-averaged back-flow velocity is not the critical factor in the formation of back-flow ripples. A measure of the frequency and duration of high magnitude velocity packets must also be considered.

Whilst little correlation was observed between bar and ripple height in these experiments, host bedform height is likely to influence ripple development under certain conditions. Because flow separation length is influenced by host bedform height, larger host bedforms will often provide a longer zone in which back-flow ripples can develop, this could be particularly important under low flow velocity conditions where ripple development is relatively slow. It is also likely that there exists a minimum host bedform height beyond which back-flow ripple formation is precluded by the small size and length of the flow separation zone which was not reached in these experiments.

Deceleration over bars is an important factor in bottomset development (Reesink & Bridge, 2009, 2011). Larger deceleration over a bar leads to enhanced suspended sediment deposition. Thus, little bottomset development is expected with low height bars relative to water depth. With a relatively weak back-flow, finer sand deposited from suspension would more easily develop back-flow ripples by allowing sediment movement by lower magnitude velocity packets. With a relatively strong back-flow, finer sand is more likely to be washed out by higher magnitude velocity packets. Where suspension fallout in the trough is minimal but a strong back-flow develops, back-flow ripples could form by reworking coarser sand already present on the bed.

Ripple types and preservation

Ripple heights varied from 1 to 20 mm; a greater range than the 3 to 10 mm found by Allen (1965) related to the difference in grain size. Ripple heights were often less than the 15 to 20 mm recorded by Johansson (1963).

Conventional back-flow ripples were either straight or sinuous crested, as observed also by Johansson (1963) and Allen (1965); they tended to be preserved in the deposits and this high preservation potential explains the prevalence of conventional back-flow ripple descriptions in the literature (e.g. Jopling, 1961; Johansson, 1963; Basumallick, 1966; Boersma *et al.*, 1968). Jopling (1961) suggested that the geometry of back-flow ripples was usually well-preserved during burial, but occasional distortions were induced by avalanching sands from the lee face of the host bedform.

As with ripples formed under steady unidirectional flow, flow sheltering (cf. Baas, 1994) can occur with back-flow ripples when a large number form. This is where individual back-flow ripples are sheltered from the flow by a ripple, which in this case is located further down-channel due to the back-flow within the lee-side eddy. This creates a ripple train with alternating ripple sizes (Fig. 7A).

Incipient back-flow ripples feature similar dimensions to incipient ripples at the early stages of ripple development in a steady unidirectional flow (Harms *et al.*, 1975; Baas, 1994, 1999) and are similar to the 'scalelike' ripples described by Allen (1965). Given enough time it is likely that they would grow into conventional back-flow ripples, but the time available is limited by the migration rate of the host bedform and the size of the lee-side eddy. The time needed for ripples to reach equilibrium with the flow is inversely related to flow velocity (Baas, 1994). Given the duration of the flume runs, and more importantly the speed of bar migration, it is unlikely that any of the ripples reached true equilibrium with the flow; this is supported by the predominance of straight and sinuous crest lines. The size of these non-equilibrium ripples may be partly related to the duration of ripple formation.

The formation of transient back-flow ripples coincided with the transition from angular to tangential cross-strata. A number of controls have been suggested which contribute to this transition, including increased deposition from suspension on the lower lee slope, the ratio of flow depth above the brink to flow depth above the trough, and turbulent eddies accelerating grain flows (Jopling, 1965; Reesink & Bridge, 2009). Transient back-flow ripple formation promotes the transition to tangential cross-strata. Transient back-flow ripples rapidly migrate from the trough up the lee slope, driving a decrease in grain size and changes in the heterogeneity of the unit bar.

Occasionally slight undulations on unit bar laminae were observed after the transition to tangential foresets (Fig. 8C). Transient back-flow ripples on unit bar foreset lamina are either completely washed out or significantly modified by grain flows and have a low preservation potential, but undulations on foreset laminea may be preserved in the deposits. Under certain flow or sediment conditions these undulations may be better preserved. Cross-stratification that may have been influenced by transient back-flow ripples has been identified in fluvial deposits (type 3 cross-strata in fig. 10, as well as fig. 13 in Boersma, 1967) and in flume studies (fig. 12A in Reesink & Bridge, 2009). These deposits often featured abundant foresets that appeared wavy or curvilinear. Boersma (1967) noted that these foresets contained finer or more poorly sorted sediment in comparison to the rectilinear foresets, as also observed in the present study. Similar structures have been found in the rock record (Fig. 8D).

Palaeoenvironmental interpretations from back-flow ripples

This research indicates that bottomsets in cross-bedded sand can form in conditions other than those proposed by Martinius & Van den Berg

(2011) for dune-related bottomset development (Fig. 5) when they form in association with unit bars or in settings where the flow over dunes changes faster than the dunes can adjust. Although these runs have examined back-flow ripples formed in the lee of unit bars, some observations may be applicable to back-flow ripples formed in dune troughs (e.g. Kirk, 1983; Martinius & Van den Berg, 2011). Dunes out of equilibrium with the flow migrating under unsteady flow conditions, such as a decreasing θ' (cf. Van den Berg & Van Gelder, 1993), could generate back-flow ripples outside the conditions suggested in Fig. 5.

When conventional back-flow ripples are restricted to the bottomset, they tend to be well-preserved and the dimensions of the preserved forms are close to those of the back-flow ripples during their formation. However, when back-flow ripples migrate rapidly or the host bedform migrates very slowly, preserved ripples become wedge shaped and extend up the host bedform foreset laminae creating fine-grained periodic climbing ripple cross-lamination (Fig. 7F).

Back-flow ripples can form over a wide range of flow velocities, contrary to earlier suggestions that they are either evidence of low flow velocities (Boersma, 1967; Nio *et al.*, 1980) or of stream velocities >0·61 m s^{-1} (Jopling, 1961). The variation in ripple structure with flow velocity make back-flow ripples potentially viable palaeovelocity indicators, although it is important to remember that these results do not precisely model riverine conditions because velocity increases were not associated with a water depth increase. At low flow velocities (<0·3 m s^{-1} in this study) incipient back-flow ripples can form and preservation depends on the transition to conventional back-flow ripples. If back-flow ripples are preserved their height is likely to be much less than a ripple of the same grain size at equilibrium with the flow due to both the limited ripple development time prior to burial and sediment transport in the trough being driven only by turbulent events. Host bedform height may influence back-flow ripple development at low flow velocities because larger bedforms will often provide a larger flow separation zone, lengthening ripple development time. At moderate flow velocities (0·3 to 0·7 m s^{-1} in this study) conventional back-flow ripples can develop. Depending on the back-flow velocity and variability, the length of the flow separation zone and the host bedform migration rate conventional back-flow ripples may or may not approach equilibrium height. At high flow velocities (>0·65 m s^{-1} in this study), the remnants of migrating transient back-flow ripples may be present as occasional undulations anywhere along the host bedform foresets.

Deducing the original height of back-flow ripples that have interfingered with the foreset lamination of the host bedform may be difficult, hindering palaeovelocity interpretation. However, interfingering suggests that the host bedform migration rate was slow relative to the migration rate of the back-flow ripples. Flow unsteadiness can lead to significant variations in bar trough deposits, particularly in shallower parts of a channel (Reesink & Bridge, 2011) and it is likely that back-flow ripple preservation in rivers may be intermittent because of flow variability. When present, structural variation in back-flow ripples preserved along the base of a cross-stratified set could be used as an indicator of flow variability during deposition. For example, during changing flow conditions conventional back-flow ripples may be preserved at the base of a cross-bed set formed by a unit bar; these may change in height as the flow conditions change (Fig. 4). Past a threshold velocity (0·65 to 0·7 m s^{-1} in these experiments) conventional back-flow ripples no longer form, instead transient back-flow ripples make undulations on unit bar cross-stratum (Fig. 8C) and there is a transition to tangential foreset laminae.

Back-flow ripple development is influenced by the flow in the trough downstream of the host bedform. Strongly three-dimensional flow, which can be induced by host bedform three-dimensionality, can lead to the creation of ripple fans or a number of ripple fan cells (Allen, 1968, 1982b). Where there is a considerable lateral component to the flow (for example, a bar front oblique to mean flow direction, close to a channel bend or tributary) back-flow ripples are likely to form oblique to the bar front (e.g. Boersma *et al.*, 1968). If lateral flow predominates and there is negligible flow separation normal current ripples may develop. These ripples can appear like back-flow ripples in cross-section of deposits (e.g. Collinson, 1970). For any palaeoenvironmental reconstruction, the orientation of ripples in relation to the mean flow direction should be assessed. Many factors including the characteristics of the sediment, host bedform height and shape, lee-side eddy and discharge variation probably alter the structure of preserved back-flow ripples, and at present most remain unquantified. Examples of this are found

in bottomsets influenced by tidal processes that can contain back-flow and co-flow ripples (Nio *et al.*, 1980; Van den Berg *et al.*, 2007), as well as parallel lamination (Van den Berg *et al.*, 2007) and climbing ripple cross-lamination (Nio *et al.*, 1980). This variation in bottomset structure has been attributed to flow reversals controlled by flood and ebb currents (Nio *et al.*, 1980; Van den Berg *et al.*, 2007) as well as wave action (Nio *et al.*, 1980). Due to the number of unquantified parameters that can influence back-flow ripple formation and structure, currently many assumptions must be made for palaeocurrent reconstructions using them. Further flume research is required to determine the effects of bar height, water depth and bottomset grain size on back-flow ripple development and geometry.

The role of unsteady flows in bedform development

As with back-flow ripple development, unsteady flow could be an important control in the development of larger bedforms. Flow conditions in rivers are often variable leading to changes in bedform geometry over time; however, bedform geometry change generally lags changes in flow conditions (Allen, 1973). If flow variation is slow, bedforms may adjust to the changing conditions so that bedform dimensions remain close to equilibrium values (Gabel, 1993). However, in rivers dominated by unsteady flows, such as arid ephemeral and semi-arid flashy rivers (e.g. Karcz, 1972; Amos *et al.*, 2004) or rivers with dam releases (e.g. Reesink & Bridge, 2011), large bedforms (for example, unit bars) will be the product of rapidly changing flow resulting in composite bed features formed and progressively modified under a wide range of discharges, never reaching equilibrium with the changing flow. Short-duration high discharge events could cause bedform growth and migration or could wash out pre-existing bedforms fully or in part, in a comparable way to high velocity packages forming or washing out back-flow ripples in the experiments described above. During low discharge conditions bedforms present on the bed could differ significantly to what would be generated under steady flow conditions. With both back-flow ripples and larger bedforms in flashy settings the relative duration of different flow conditions (high and low velocity packages in a bar lee, or flash flood and low discharge conditions in a semi-arid river) will be as or more important than mean flow conditions.

CONCLUSIONS

Back-flow ripples formed in the lee-side eddy of a unit bar over a wide range of flow velocities. Millimetre high *incipient back-flow ripples* formed at low velocities. Well-developed *conventional back-flow ripples* formed at moderate velocities and *transient back-flow ripples* formed and migrated up the unit bar lee slope at higher velocities. Although no record of incipient back-flow ripples was preserved in the deposits, conventional back-flow ripples had a high preservation potential and formed characteristic structures within the bar deposits. Evidence of transient back-flow ripples was occasionally preserved as undulations on foreset laminae. These ripples influenced the grain size and sorting within the host bedform by transporting sediment from the trough up the lee face.

The very variable flow velocity near the bed in the lee of the bar allowed back-flow ripples to form at lower mean back-flow velocities than anticipated. The velocity variation was caused by vortex shedding, wake flapping and changes in the size of and turbulence within the flow separation zone resulting from superimposed bedforms on the bar approaching the bar crest. In this context mean back-flow velocity may be less important for back-flow ripple formation than the magnitude and duration of high velocity packages. These packets cause the transience of the back-flow ripples at higher flow velocities.

Burial of back-flow ripples by the advancing host bedform limits the time available for the bedforms to develop; this as well as the limited length of the lee-side eddy and the velocity variability within it means that back-flow ripples will rarely reach equilibrium and their size and shape may be an indicator of depositional conditions (unlike equilibrium ripples where size is related more strongly to sediment grain size). The shape of back-flow ripples in these experiments changed with flow velocity, suggesting that it may be possible to use the morphology of back-flow ripples preserved within ancient deposits as an indicator of palaeoflow velocity in cases where ripples had migration directions parallel but opposed to the mean flow direction. Changes in back-flow ripple morphology within

single cross-strata sets would indicate flow variability.

ACKNOWLEDGEMENTS

This work was supported by the Natural Environment Research Council (grant numbers NE/L50158X/1, NE/H524506/1). The data used in this publication are available on request to the authors. Thanks to field assistants Eleanor Keightley and Matthew Heaver, and to reviewers Arjan Reesink and Janrik Van den Berg for their comments and suggestions.

ABBREVIATIONS

D_{50}	Median size
D_*	Non-dimensional particle parameter (cf. Van den Berg & Van Gelder, 1993)
P_v	Periodicity of vortex shedding
P_w	Periodicity of wake flapping
U_b	Mean flow velocity above the unit bar brink
u	Downchannel velocity component
$\bar{u}$	Time averaged downchannel velocity component in a velocity profile
u'	Instantaneous deviation from mean downchannel velocity
V	Mean back-flow velocity
V_{rms}	Root mean square of back-flow velocity
x	Direction parallel to the channel axis with distance measured from the upstream end of the test channel (see Fig. 2)
x_r	Length of flow separation zone
y	Direction across flow from left to right looking downstream (see Fig. 2)
$\bar{y}$	Time averaged cross-channel velocity component
z	Direction perpendicular to the solid bed of the test channel (see Fig. 2)
$\bar{z}$	Time averaged vertical velocity component
σ	Standard deviation
θ'	Modified mobility parameter (cf. Van den Berg & Van Gelder, 1993)

REFERENCES

Abouessa, A., **Pelletier, J.**, **Duringer, P.**, **Schuster, M.**, **Schaeffer, P.**, **Métais, E.**, **Benammi, M.**, **Salem, M.**, **Hlal, O.**, **Brunet, M.**, **Jaeger, J.J.** and **Rubino, J.L.** (2012) New insight into the sedimentology and stratigraphy of the Dur At Talah tidal-fluvial transition sequence (Eocene-Oligocene, Sirt Basin, Libya). *J. Afr. Earth Sci.*, **65**, 72–90.

Allen, J.R.L. (1965) Sedimentation to the lee of small underwater sand waves: an experimental study. *J. Geol.*, **73**, 95–116.

Allen, J.R.L. (1968) *Current Ripples, Their Relation to Patterns of Water and Sediment Motion*. North-Holland Publishing Company, Amsterdam, 433 pp.

Allen, J.R.L. (1973) Phase differences between bed configuration and flow in natural environments, and their geological relevance. *Sedimentology*, **20**, 323–329.

Allen, J.R.L. (1980) Sand waves: a model of origin and internal structure. *Sed. Geol.*, **26**, 281–328.

Allen, J.R.L. (1982a) *Sedimentary Structures: Their Character and Physical Basis, Volume 1*. Elsevier, Amsterdam, 593 pp.

Allen, J.R.L. (1982b) *Sedimentary Structures: Their Character and Physical Basis, Volume 2*. Elsevier, Amsterdam, 663 pp.

Allen, J.R.L. and **Narayan, J.** (1964) Cross-stratified units, some with silt bands, in the Folkestone Beds (lower Greensand) of Southeast England. *Geol. Mijnbouw*, **43**, 451–461.

Amos, K.J., **Alexander, J.**, **Horn, A.**, **Pocock, G.D.** and **Fielding, C.R.** (2004) Supply limited sediment transport in a high-discharge event of the tropical Burdekin River, North Queensland, Australia. *Sedimentology*, **51**, 145–162.

Ashworth, P.J., **Best, J.L.**, **Roden, J.E.**, **Bristow, C.S.** and **Klaassen, G.J.** (2000) Morphological evolution and dynamics of a large, sand braid-bar, Jamuna River, Bangladesh. *Sedimentology*, **47**, 533–555.

Baas, J.H. (1994) A flume study on the development and equilibrium morphology of current ripples in very fine sand. *Sedimentology*, **41**, 185–209.

Baas, J.H. (1999) An empirical model for the development and equilibrium morphology of current ripples in fine sand. *Sedimentology*, **46**, 123–138.

Baas, J.H., **Best, J.L.** and **Peakall, J.** (2011) Depositional processes, bedform development and hybrid bed formation in rapidly decelerated cohesive (mud-sand) sediment flows. *Sedimentology*, **58**, 1953–1987.

Basumallick, S. (1966) Size differentiation in a cross-stratified unit. *Sedimentology*, **6**, 35–68.

Bennett, S.J. and **Best, J.L.** (1995) Mean flow and turbulence structure over fixed, two-dimensional dunes: implications for sediment transport and bedform stability. *Sedimentology*, **42**, 491–513.

Best, J. (2005) The fluid dynamics of river dunes: a review and some future research directions. *J. Geophys. Res.*, **110**, F04S02. doi:10.1029/2004JF000218.

Best, J., **Blois, G.**, **Barros, J.** and **Christensen, K.** (2013) *The Dynamics of Bedform Amalgamation: New Insights from a Very Thin Flume*. Proceedings of the Marine and River Dunes Conference 2013, Bruges, Belgium.

Boersma, J.R. (1967) Remarkable types of mega cross-stratification in the fluviatile sequence of a subrecent distributary of the Rhine. Amerongen; The Netherlands. *Geol. Mijnbouw*, **46**, 217–235.

Boersma, J.R., **van de Meene, E.A.** and **Tjalsma, R.C.** (1968) Intricated cross-stratification due to interaction of a mega ripple with its lee-side system of backflow ripples (upper-pointbar deposits, Lower Rhine). *Sedimentology*, **11**, 147–162.

Carling, P.A. and **Glaister, M.S.** (1987) Rapid deposition of sand and gravel mixtures downstream of a negative step:

the role of matrix-infilling and particle-overpassing in the process of bar-front accretion. *J. Geol. Soc. London*, **144**, 543–551.

Carling, P.A., **Williams, J.J.**, **Gölz, E.** and **Kelsey, A.D.** (2000) The morphodynamics of fluvial sand dunes in the River Rhine, near Mainz, Germany. II. Hydrodynamics and sediment transport. *Sedimentology*, **47**, 253–278.

Casshyap, S.M. and **Kumar, A.** (1987) Fluvial architecture of the Upper Permian Raniganj coal measure in the Damodar basin, Eastern India. *Sed. Geol.*, **51**, 181–213.

Collinson, J.D. (1968) Deltaic sedimentation units in the Upper Carboniferous of Northern England. *Sedimentology*, **10**, 233–254.

Collinson, J.D. (1970) Bedforms of the Tana River, Norway. *Geogr. Ann. Ser. A Phys. Geogr.*, **52**, 31–56.

Dasgupta, P. and **Bandyopadhyay, S.** (2008) Carbonate aeolianites of western Saurashtra, India: experimental decipherment of the depositional mechanisms. *Sedimentology*, **55**, 1361–1374.

De Mowbray, T. and **Visser, M.J.** (1984) Reactivation surfaces in subtidal channel deposits, Oosterschelde, southwest Netherlands. *J. Sed. Petrol.*, **54**, 811–824.

Fernandez, R., **Best, J.** and **López, F.** (2006) Mean flow, turbulence structure, and bed form superimposition across the ripple-dune transition. *Water Resour. Res.*, **42**, W05406. doi: 10.1029/2005WR004330.

Gabel, S.L. (1993) Geometry and kinematics of dunes during steady and unsteady flows in the Calamus River, Nebraska, USA. *Sedimentology*, **40**, 237–269.

George, G.T. (2000) Characterisation and high resolution sequence stratigraphy of storm-dominated braid delta and shoreface sequences from the Basal Grit Group (Namurian) of the South Wales Variscan peripheral foreland basin. *Mar. Pet. Geol.*, **17**, 445–475.

Gradzinski, R. (1970) Sedimentation of dinosaur-bearing Upper Cretaceous deposits of the Nemegt Basin, Gobi Desert. *Palaeontol. Pol.*, **21**, 147–229.

Gustavson, T.C., **Ashley, G.M.** and **Boothroyd, J.C.** (1975) Depositional sequences in glaciolacustrine deltas. In: *Glaciofluvial and Glaciolacustrine Sedimentation* (Eds A.V. Jopling and B.C. McDonald), *SEPM Spec. Publ.*, **23**, 264–280.

Hardy, R.J., **Best, J.L.**, **Lane, S.N.** and **Carbonneau, P.E.** (2009) Coherent flow structures in a depth-limited flow over a gravel surface: the role of near-bed turbulence and influence of Reynolds number. *J. Geophys. Res.*, **114**, F01003. doi: 10.1029/2007JF000970.

Harms, J.C., **Southard, J.B.**, **Spearing, D.R.** and **Walker, R.G.** (1975) Depositional environments as interpreted from primary sedimentary structures and stratification sequences. *SEPM Short Course Notes*, **2**, 161.

Helm, D.G. (1971) Succession and sedimentation of glacigenic deposits at Hendre, Anglesey. *Geol. J.*, **7**, 271–298.

Hunter, R.E. (1985) Subaqueous sand-flow cross strata. *J. Sed. Res.*, **55**, 886–894.

Johansson, C.E. (1963) Orientation of pebbles in running water. A laboratory study. *Geogr. Ann.*, **45**, 85–112.

Jopling, A.V. (1961) Origin of regressive ripples explained in terms of fluid-mechanic processes. *U.S. Geol. Surv. Prof. Pap.*, **424-D**, 15–17.

Jopling, A.V. (1965) Hydraulic factors controlling the shape of laminae in laboratory deltas. *J. Sed. Petrol.*, **35**, 777–791.

Karcz, I. (1972) Sedimentary structures formed by flash floods in southern Israel. *Sed. Geol.*, **7**, 161–182.

Kirk, M. (1983) Bar development in a fluvial sandstone (Westphalian 'A'), Scotland. *Sedimentology*, **30**, 727–742.

Kostaschuk, R. (2000) A field study of turbulence and sediment dynamics over subaqueous dunes with flow separation. *Sedimentology*, **47**, 519–531.

Kostic, B. and **Aigner, T.** (2004) Sedimentary and poroperm anatomy of shoal-water carbonates (Muschelkalk, South-German Basin): an outcrop-analogue study of inter-well spacing scale. *Facies*, **50**, 113–131.

Liu, Y., **Liang, X.S.** and **Weisberg, R.H.** (2007) Rectification of the bias in the wavelet power spectrum. *J. Atmos. Ocean Tech.*, **24**, 2093–2102.

Livera, S.E. and **Leeder, M.R.** (1981) The Middle Jurassic Ravenscar Group ('deltaic series') of Yorkshire: recent sedimentological studies as demonstrated during a field meeting 2–3 May 1980. *Proc. Geol. Assoc.*, **92**, 241–250.

Macdonald, R.G., **Alexander, J.**, **Bacon, J.C.** and **Cooker, M.J.** (2013) Variations in the architecture of hydraulic jump unit bar complexes on non-eroding beds. *Sedimentology*, **60**, 1291–1312.

Maddux, T.B., **Nelson, J.M.** and **McLean, S.R.** (2003) Turbulent flow over three-dimensional dunes: 1. free surface and flow response. *J. Geophys. Res.*, **108**, 6009. doi:10.1029/2003JF000017.

Martinius, A.W. and **Van den Berg, J.H.** (2011) *Atlas of Sedimentary Structures in Estuarine and Tidally-Influenced River Deposits of the Rhine-Meuse-Scheldt System*. European Association of Geoscientists & Engineers, Houten, 298 pp.

McCabe, P.J. and **Jones, C.M.** (1977) Formation of reactivation surfaces within superimposed deltas and bedforms. *J. Sed. Petrol.*, **47**, 707–715.

Miller, M.C., **McCave, I.N.** and **Komar, P.D.** (1977) Threshold of sediment motion under unidirectional currents. *Sedimentology*, **24**, 507–527.

Nezu, I. and **Nakagawa, H.** (1993) *Turbulence in Open-Channel Flows*. IAHR Monograph A.A. Balkema, Rotterdam, 281 pp.

Nezu, I., **Nakagawa, H.** and **Tominaga, A.** (1985) Secondary currents in a straight channel flow and the relation to its aspect ratio. In: *Turbulent Shear Flows 4* (Eds L.J.S. Bradbury, F. Durst, B.E. Launder, F.W. Schmidt and J.H. Whitelaw), pp. 246–260. Springer-Verlag, Berlin.

Nielsen, L.H. and **Johannessen, P.N.** (2009) Facies architecture and depositional processes of the Holocene-Recent accretionary forced regressive Skagen spit system, Denmark. *Sedimentology*, **56**, 935–968.

Nio, S.D., **van den Berg, J.H.**, **Goesten, M.** and **Smulders, F.** (1980) Dynamics and sequential analysis of a mesotidal shoal and intershoal channel complex in the Eastern Scheldt (southwestern Netherlands). *Sed. Geol.*, **26**, 263–279.

Omidyeganeh, M. and **Piomelli, U.** (2013) Large-eddy simulation of three-dimensional dunes in a steady, unidirectional flow. Part 1. Turbulence statistics. *J. Fluid Mech.*, **721**, 454–483.

Paarlberg, A.J., **Dohmen-Janssen, C.M.**, **Hulscher, S.J.M.H.** and **Termes, P.** (2007) A parameterization of flow separation over subaqueous dunes. *Water Resour. Res.*, **43**, W12417. doi:10.1029/2006WR005425.

Reesink, A.J.H. and **Bridge, J.S.** (2007) Influence of superimposed bedforms and flow unsteadiness on formation of cross strata in dunes and unit bars. *Sed. Geol.*, **202**, 281–296.

Reesink, A.J.H. and **Bridge, J.S.** (2009) Influence of bedform superimposition and flow unsteadiness on the formation

of cross strata in dunes and unit bars — part 2, further experiments. *Sed. Geol.*, **222**, 274–300.

Reesink, A.J.H. and **Bridge, J.S.** (2011) Evidence of bedform superimposition and flow unsteadiness in unit-bar deposits, South Saskatchewan River, Canada. *J. Sed. Res.*, **81**, 814–840.

Reesink, A.J.H., **Parsons, D.R.** and **Thomas, R.E.** (2014) *Sediment Transport and Bedform Development in the Lee of Bars: Evidence from Fixed- and Partially-Fixed Bed Experiments*. River Flow 2014, Lausanne, Switzerland.

Saunderson, H.C. and **Jopling, A.V.** (1980) Palaeohydraulics of a tabular, cross-stratified sand in the Brampton Esker, Ontario. *Sed. Geol.*, **25**, 169–188.

Schatz, V. and **Herrmann, H.J.** (2006) Flow separation in the lee side of transverse dunes: a numerical investigation. *Geomorphology*, **81**, 207–216.

Shugar, D.H., **Kostaschuk, R.**, **Best, J.L.**, **Parsons, D.R.**, **Lane, S.N.**, **Orfeo, O.** and **Hardy, R.J.** (2010) On the relationship between flow and suspended sediment transport over the crest of a sand dune, Río Paraná, Argentina. *Sedimentology*, **57**, 252–272.

Simpson, R.L. (1989) Turbulent boundary-layer separation. *Annu. Rev. Fluid Mech.*, **21**, 205–234.

Smith, S.A. and **Edwards, R.A.** (1991) Regional sedimentological variation in Lower Triassic fluvial conglomerates (Budleigh Salterton Pebble Beds), southwest England: some implications for palaeogeography and basin evolution. *Geol. J.*, **26**, 65–83.

Sohn, Y.K., **Park, J.B.**, **Khim, B.K.**, **Park, K.H.** and **Koh, G.W.** (2003) Stratigraphy, petrochemistry and Quaternary depositional record of the Songaksan tuff ring, Jeju Island, Korea. *J. Volcanol. Geoth. Res.*, **119**, 1–20.

Terwindt, J.H.J. (1971) Sand waves in the Southern Bight of the North Sea. *Mar. Geol.*, **10**, 51–67.

Theakstone, W.H. (1976) Glacial lake sedimentation, Austerdalsisen, Norway. *Sedimentology*, **23**, 671–688.

Tillman, R.W. and **Ellis, C.W.** (1968) Reversed-climbing ripples and sand-wave deposition in Arkansas River: abstract. *Am. Assoc. Pet. Geol. Bull.*, **52**, 552.

Torrence, C. and **Compo, G.P.** (1998) A practical guide to wavelet analysis. *Bull. Am. Meteorol. Soc.*, **79**, 61–78.

Van Beek, J.L. and **Koster, E.A.** (1972) Fluvial and estuarine sediments exposed along the Oude Maas (The Netherlands). *Sedimentology*, **19**, 237–256.

Van den Berg, J.H. and **Van Gelder, A.** (1993) A new bedform stability diagram, with emphasis on the transition of ripples to plane bed in flows over fine sand and silt. In: *Alluvial Sedimentation* (Eds M. Marzo and C. Puigdefàbregas), *Int. Assoc. Sedimentol. Spec. Publ.*, **17**, 11–21.

Van den Berg, J.H., **Boersma, J.R.** and **van Gelder, A.** (2007) Diagnostic sedimentary structures of the fluvial-tidal transition zone – evidence from deposits of the Rhine and Meuse. *Geol. Mijnbouw*, **86**, 287–306.

Venditti, J.G. (2007) Turbulent flow and drag over fixed two- and three-dimensional dunes. *J. Geophys. Res.*, **112**, F04008. doi:10.1029/2006JF000650.

Yalin, M.S. (1964) Geometrical properties of sand waves. *Proc. Am. Soc. Civ. Eng.*, **90**, 105–119.

Yalin, M.S. (1985) On the determination of ripple geometry. *J. Hydraul. Eng.*, **111**, 1148–1155.

Zhang, J., **Qin, L.** and **Zhang, Z.** (2008) Depositional facies, diagenesis and their impact on the reservoir quality of Silurian sandstones from Tazhong area in central Tarim Basin, western China. *J. Asian Earth Sci.*, **33**, 42–60.

Manuscript received 11 June 2014; revision accepted 5 March 2015